이학박사학위논문

염색체 방추사 부착점에서 미세소관 부착과 세포분열 체크포인트 신호전달로 이어지는 **BubR1** 기능에 대한 연구

BubR1 in the Coordination of Kinetochore-Microtubule Attachment and Spindle Assembly Checkpoint Signaling

2016 년 2 월

서울대학교 대학원
생명과학부

박인애

ABSTRACT

BubR1 in the Coordination of Kinetochore-Microtubule Attachment and Spindle Assembly Checkpoint Signaling

Inai Park

School of Biological Sciences

Seoul National University

BubR1 is a key protein constituting the mitotic checkpoint complex (MCC). During mitosis, the spindle assembly checkpoint (SAC) acts to delay anaphase onset until all chromosomes are attached to mitotic spindles at kinetochores. The SAC works through generation of MCC, which inhibits the anaphase-promoting complex/cyclosome E3 ligase (APC/C) in the cytoplasm. This study addresses on first, how BubR1 coordinated kinetochore-microtubule (KT-MT) attachments and SAC signaling. Secondly, it also addresses on how a regulator in mitosis, tumor suppressor BRCA2 serves as a signaling platform during SAC.

In order to understand the physiological role of BubR1 acetylation, acetylation deficient knock-in mice (*K243R/+*) were generated. After 60 weeks, 38% of mice spontaneously developed tumors at various tissues. *K243R/+* Mouse Embryonic Fibroblasts (MEFs) were highly aneuploid and had weakened SAC. At kinetochores, unstable KT-MT attachments were observed due to reduced recruitment of PP2AB56a. Insufficient amount of PP2AB56a could not counterbalance the excessive Aurora B activity at kinetochores. All together, unstable KT-MT attachment and failure in maintaining MCC formed in mitosis led to accumulation of chromosome instability (CIN) in *K243R/+*. These CIN manifested in various forms in the acetylation deficient mice generated a mutation-prone cellular environment favoring tumorigenesis.

Previous works have shown that in prometaphase, BubR1 acetylation occurs at kinetochores, only if BRCA2 is present to support the BubR1-P300/CBP-associated factor (PCAF) interaction (Choi et al., 2012). My research showed that BubR1 was deacetylated when SAC was silenced. Deacetylation of BubR1 was a cue to SAC silencing, as cells expressing acetylation mimetic form of BubR1 could not exit mitosis after the metaphase delay. Also, acetylation of BubR1 diminished when SAC silencing was mimicked in mitotic cells. Deacetylation of BubR1 was

mediated by class I HDACs, and BRCA2 was needed for HDACs to interact with BubR1 at prometaphase. Hence, one can conclude that BRCA2 not only regulates BubR1 acetylation, but it presents the acetylated BubR1 to HDACs at prometaphase for deacetylation. Analysis on the BRCA2 complex in mitosis suggested that BRCA2 acts as a signaling platform within the SAC signaling network by specifying the interaction and localization of essential proteins at kinetochores.

In essence, my study provides further insight into the following key questions in mitosis. First, the question of how KT-MT attachment is sensed and relayed to SAC was further explained by elucidating the role of BubR1 in coordinating KT-MT attachment and SAC signaling. Second, the question of how complex SAC signaling is punctually regulated by multiple proteins during metaphase to anaphase transition was addressed through elucidating the role of BRCA2 as a scaffold for BubR1 acetylation/deacetylation at kinetochores.

Key words: spindle assembly checkpoint (SAC), BubR1, tumorigenesis, SAC signaling, KT-MT attachment

Student number: 2011-20330

CONTENTS

LIST OF FIGURES

LIST OF TABLES

I. INTRODUCTION

I-1. Mitosis and chromosome instability (CIN)

The cell cycle is a series of events that allows cells to grow and divide. It is divided into three main stages; in the order of interphase, mitosis and cytokinesis. During interphase, the genetic material replicates and the organelles prepare for division. In mitosis, genetic material is distributed and the cleavage of cytoplasmic content during cytokinesis produces two daughter cells. The oscillation in the activity of specific Cyclins and Cyclin-dependent kinases together supports the directional flow into each events of the cell cycle (Malumbres and Barbacid, 2009). The conserved E3-ubiquitin ligase in eukaryotes called anaphase promoting complex /cyclosome (APC/C) targets numerous key proteins through ubiquitination so that they are degraded by 26S proteasome at right place and time to drive the cell cycle. Such targeted substrates of APC/C include Cyclins A/B, Geminin, Polo/Aurora kinases, Cdc20, BubR1 and Securin (Pines, 2011). Substrate specificity of APC/C during cell cycle is determined by interaction with either co-activators Cdh1 in interphase or Cdc20 in mitosis.

In mitosis, APC/C-Cdc20 co-activator complex is activated primarily by Cyclin-Cdk1 dependent phosphorylation. Non-phosphorable APC/C mutant by Cdc28 (Cdk1) is defective in performing Cdc20 dependent activity such as ubiquitinating Cyclin B (Rudner et al., 2000) and phosphorylation by

Cdk1 is sufficient for increasing binding of MCC to Cdc20 *in vivo* (Kraft et al., 2003). It is important that activity of APC/C-Cdc20 is regulated to allow timely degradation of Securin and Cyclin B for proper segregation of sister chromatids. In order to make this happen, inappropriately attached or unattached microtubules are monitored by spindle assembly checkpoint (SAC) proteins which assemble at kinetochores (Lara-Gonzalez et al., 2012). Thus, APC/C activity in mitosis is strictly monitored by SAC.

If dividing cells experience failure in SAC, the chances of chromosome mis-segregation increase, generating aneuploid (abnormal number of chromosomes, termed first in 1922 by Tackholm) cells (Fig.1). Acquiring more or less chromosomes due to problems in SAC result to a condition in which cells harbor unstable DNA content, or Chromosome instability (CIN). CIN could be manifested in various forms such as change in structures (e.g. fusion and internal gene deletion) or numbers of chromosomes (e.g. loss and duplication).

Figure 1

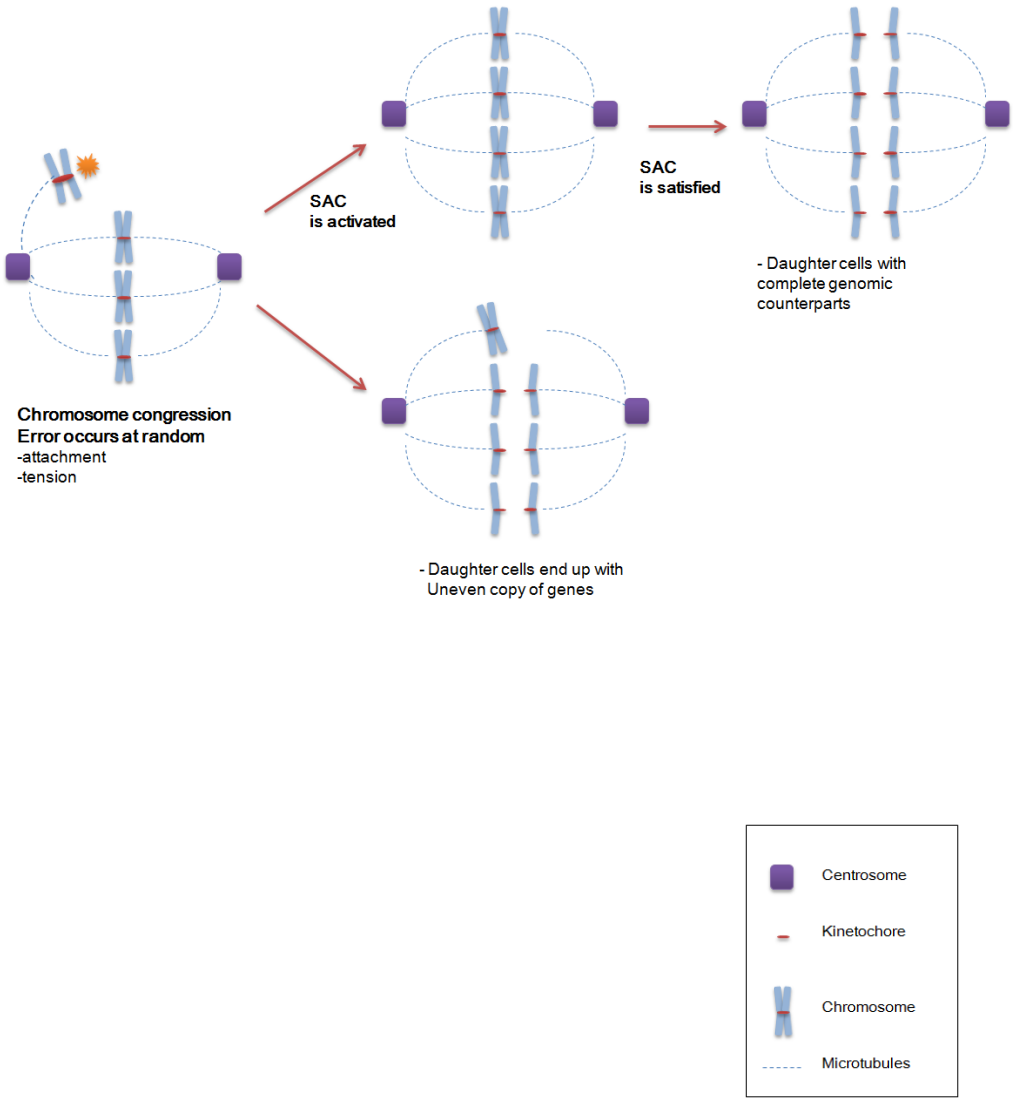
SAC
is activated
SAC
is satisfied
- Daughter cells with
complete genomic
counterparts
Chromosome congression
Error occurs at random
-attachment
-tension
- Daughter cells end up with
Uneven copy of genes
Centrosome
Kinetochore
Chromosome
Microtubules

Fig.1 SAC and chromosome segregation

A schematic diagram on the fate of chromosomes in mitosis.

An unattached kinetochore elicits SAC. **(Top)** When SAC is activated, chromosome segregation is corrected in mitosis and daughter cells receive equal copies of genes. **(Bottom)** Failure in SAC affects daughter cells to end up with uneven copy of genes which may result to cell death or become cancerous.

The effect of aneuploidy at an organism or individual level is detrimental, leading to embryonic lethality, yet with one exception of carrying trisomy at chromosome 21 (known as Down syndrome). The effect of carrying somatic cell aneuploidy maybe severe, as evaluated from the examples of human patients with mosaic variated aneuploidy (MVA) syndrome. The MVA patients carry mutations in a SAC protein gene, *BubR1*, and this symptom is characterized by mosaic aneuploidies in multiple different chromosomes and tissues. Overt features include microcephaly, early childhood cancer and mental retardation (Hanks et al., 2004). In the case of budding yeasts engineered to be disomic for one or two chromosomes, aneuploidy causes delay in G_1 phase, inhibiting proliferation (Stingeles et al., 2012; Torres et al., 2007).

On the other hand, over 90% of solid tumors are highly aneuploid with typical karyotypes ranging from 40 to 60 chromosomes on average (http://cgap.nci.nih.gov/chromosomes/mitelman). As CIN is frequently detected in human solid tumor masses, one can infer that there is a high correlation between CIN and cancer.

I-2. Mouse models for CIN

In order to understand how aneuploidy could affect tumorigenesis, mouse models which could inflict aneuploidy were generated and analyzed. These mouse models were generated by mutating or regulating transcription of the genes involved in SAC such as *Mad2, Hec1, Bub3, CENP-E, Plk1* and *BubR1* (Schvartzman et al., 2010).

One of the early models include transgenic mice over expressing Mad2, using the doxycycline inducible system. The mouse embryonic fibroblasts (MEFs) from these Mad2 over expressing mice take longer time to complete mitosis, with lagging chromosomes and chromosome bridges, resulting in both aneuploidy and tetraploidy. Furthermore, the mice show wide spectrum of tumors including hepatomas, lung adenomas and lymphomas at the latency of 12 months. When neoplastic transformation occurs, Mad2 is no longer needed to be over expressed; indicating CIN could be an early and transient oncogenic event (Sotillo et al., 2007).

On the contrary, Weaver et al. showed that aneuploidy could act either as oncogenic or tumor-suppressive through the analysis of Centromere-associated Protein-E (CENP-E) knock-out mice. CENP-E is a mitosis specific motor protein which acts in maintaining end-on attachments between microtubules and kinetochores. Reduction in CENP-E results in the accumulation of aneuploidy *in vitro* and *in vivo*. In CENP-$E^{+/-}$ mice,

spontaneous tumorigenesis takes place in liver and blood cells. But when CENP-E$^{+/-}$ mice are challenged with carcinogen, dimethyl benzanthracene (DMBA), the whole number of incidence of tumors decrease. Also, when these mice are intercrossed with p19/ARF$^{-/-}$, elevated aneuploidy owing to CENP-E knockout increases the average tumor-free survival of p19/ARF$^{-/-}$ animals from 60 days to 90 days (Weaver et al., 2007). Interestingly, in this model, aneuploidy does drive spontaneous tumorigenesis, but aneuploidy also suppresses tumorigenesis when circumstances favorable to tumor formation are made by chemical or genetic induction.

In essence, previous studies have shown that deregulated expression or mutation of mitotic checkpoint genes lead to various grade of aneuploidy in mice. Yet, consequences varied; some develop tumors under exposure to carcinogens or are completely tumor-free (Schvartzman et al., 2010), which I think provided an inconclusive answer to the question of whether aneuploidy is a negative or a positive cue to tumorigenesis.

BubR1 mouse models

What do we know so far, when BubR1 is constitutively mutated or disrupted in mouse models? In 2004, BubR1 knockout mice were generated using the gene trapping method to insert the neomycin cassette between exon 1 and 2 of *mBubR1*, disrupting the allele. *BubR1*$^{-/-}$ mice are embryonic lethal at Embryonic Stage 6.5 days, due to apoptosis, unable to be characterized (Wang et al., 2004). *BubR1*$^{+/-}$ MEFs express ~50% at the protein level, and are defective in SAC activation, as levels of Cdc20 and Securin are low. In addition, incidence of polyploidy and micronuclei increase after cell divisions (Dai et al., 2004). Haploinsufficient *BubR1*$^{+/-}$ mice lack obvious abnormal phenotypes but harbor splenomegaly and show abnormal megakaryopoiesis. But when the mice are challenged with carcinogen azoxymethane (AOM), they develop colon and lung adenoma at high incidence (Dai et al., 2004).

Unlike the tumor-prone phenotype seen from *BubR1*$^{+/-}$ mice, mutant mice generated to express BubR1 at graded levels show unanticipated roles of BubR1 in regulating aging. Expression of BubR1 was gradually reduced from the normal level (+/+) to zero by the use of the wild type (+), knock out (-) and hypomorphic alleles (H). When BubR1 level is expressed at the level around 10% of the normal (*BubR1*$^{-/H}$), the mice die within several hours due to respiratory problems. But the mice expressing about 29% of the protein

(*BubR1*$^{H/H}$, hypomorphic), have the life span of 6 months and develop aging related phenotypes such as dwarfism, lordokyphosis, cataracts, loss of subcutaneous fat and impaired wound healing. At cellular level, *BubR1*$^{H/H}$ MEFs show shortened duration of mitotic arrest under the exposure to nocodazole, high incidence of aneuploidy and grow slow in culture, going into senescence (Baker et al., 2004). However, the hypomorphic mice do not develop spontaneous tumors.

All together, mice with mutations in BubR1 vary in characteristics. Even though both mouse models commonly possess aneuploidy at cellular level, they show overtly different phenotypes. It is still unclear from analyzing these previous mouse models in that what aspects of BubR1 and whether aneuploidy resulting from defective SAC directly affect tumorigenesis. Also, one cannot rule out the possibility that by over expressing or down regulating the cellular expression level of genes throughout the cell cycle, none mitotic consequences could have affected the phenotype of mice. In effect, insufficiency of BubR1 causes accumulation of senescence markers and growth arrest. Also, several checkpoint genes including *Mad2* are reported to be regulated under the control of E2F transcription factor from G1 to S phase (Lovino et al., 2006).

Therefore, there is a need for **a better mouse model** which could

1) **Specifically access the correlation between SAC regulation and**

tumorigenesis and further

2) **Elucidate the roles of BubR1 in SAC.**

I-3. Spindle assembly checkpoint (SAC) activity and regulation

In eukaryotes, SAC is a safety mechanism which monitors kinetochore-microtubule (KT-MT) attachment during prometaphase to ensure faithful segregation of chromosomes by delaying the entry into anaphase (Musacchio and Salmon, 2007). Some essential checkpoint proteins include Mad1, Mad2, BubR1 (MAD3 in yeast), Bub3, Bub1 and Mps1. These genes were first identified in 1991, through a genetic screen in budding yeast for sensitivity to spindle poisons. Loss-of-function mutants of such mitotic arrest deficient (MAD) and budding uninhibited by benzimidazole (BUB) genes are viable as long as the cell division proceeds (Benezra et al., 2010). The checkpoint proteins Mad2, BubR1, Bub3 and Cdc20 form the MCC, enabling SAC to be effective upon activation.

Signal generation at kinetochore

Spindle assembly is a dynamic yet error-prone process, involving multiple rounds of microtubule attachment and detachment at individual kinetochores (Dick et al., 2013). For instance, when the sister kinetochores

attach to microtubule spindles emanating from a single spindle pole (syntelic attachment) or when only one of the sister kinetochores attach to the mitotic spindle (monotelic attachment), SAC is activated. SAC is very sensitive, enough to respond to a single unattached kinetochore to delay anaphase onset for several hours, as seen from laser ablation experiments from Ptk1 cells (Rieder et al., 1995) and to loss of tension between sister chromatid kinetochores. The number of unattached kinetochores are proportional to the strength of SAC signaling (Dick and Gerlich, 2013; Collin et al., 2013) and unattached kinetochores are critical to priming the catalysis of MCC (Kulukian, A. et al., 2009).

During prometaphase, SAC proteins and Cdc20 accumulate at outer kinetochore to generate the wait-anaphase signal and inhibit APC/C-Cdc20 activator complex to block degradation of Cyclin B and Securin (Lara-Gonzalez et al., 2012).The kinetochore, in which MCC assembles, is a built on CENP-A marked centromeric chromatin (Perpelescu and Fukagawa, 2011). Specifically, outer kinetochore is constituted by the KMN network comprised of KNL1, Mis12 and Ndc80 sub complexes. The KMN network has the prime role in allowing load-bearing attachments to dynamic microtubules (Joglekar and Deluca, 2009). In addition, KNL1 and its binding partner Zwint act as a scaffold for the SAC proteins (Bub1, BubR1, Bub3, Mad1, Mad2, the RZZ (Rod/Zw10/Zwilch) complex and Spindly) (Varma

and Salmon, 2012). Another complex at the outer kinetochore needed for microtubule attachment is the RZZ complex, unique to the metazoan cells. The RZZ complex plays an essential role in SAC, by recruiting Mad1 and Mad2 to unattached kinetochores (Karess et al., 2005).

MCC, inhibitor of SAC

How is then, the mechanical sensor at unattached kinetochores is converted to chemical signaling to inhibit APC/C in prometaphase? In other words, what is the nature of the wait-anaphase signal generated from unattached kinetochores? The best understanding up-to-date comes from the 'Mad2 template model'. The fluorescence recovery after photo bleaching (FRAP) analysis of GFP tagged proteins showed that all MCC components cycle on and off from the kinetochores with high turnover rates. This implies that MCC is dynamically created at kinetochores (Howell et al., 2004). In this theory, Mad2 acts as the template for generation of Mad2-Cdc20 complexes, an initial step in MCC assembly. In short, Mad2 adopts two distinct structural conformations: open (o-Mad2) and closed (c-Mad2) conformations. Upon mitotic entry, Mad1 and c-Mad2 form a hetero tetrameric complex at the kinetochores (Schuyler et al., 2012). Then cytosolic o-Mad2 are recruited to the kinetochore bound Mad1-c-Mad2, dimerizing with the Mad1 bound c-Mad2. This newly recruited o-Mad2 is

activated and leaves the kinetochore to capture Cdc20, creating c-Mad2-Cdc20 complex (De-antoni et al., 2005). The c-Mad2-Cdc20 complex auto-amplifies the signal by converting more o-Mad2 into c-Mad2 (Luo et al., 2002). Thus, c-Mad2-Mad1 acts as a template, by catalyzing the conversion of o-Mad2 to compatible c-Mad2 for Cdc20 interaction. Whereas the first sub complex of MCC (c-Mad2-Cdc20) is actively generated from kinetochores, the second sub complex of the MCC, BubR1-Bub3 complex exists throughout the cell cycle (Chen et al., 2002).

Through the analysis of crystal structure on MCC in yeast cells, much on the protein-protein interaction within the MCC is unraveled. Mad2 is necessary for BubR1-Cdc20 interaction and the KEN1 box in BubR1 is also needed for Mad2-Cdc20 binding (Davenport et al., 2006; Nilsson et al., 2008; Lara-Gonzalez et al., 2011). Although the yeast MCC structure includes only N-terminus of hBubR1 (MAD3), it is clear that 1) TPR domain of BubR1 interacts with Cdc20, 2) KEN box forms a Helix-loop-helix structure to interact with Mad2-Cdc20, 3) c-Mad2 interacts with BubR1 and Cdc20 through the same domain that interacts with o-Mad2 and 4) BubR1 acts as a pseudo-substrate inhibitor of APC/C by occupying the substrate recognition module within the APC/C, disabling APC/C to accept substrates in mitosis (Chao et al., 2012). These MCC proteins bind in approximately 1:1:1:1 sub-stoichiometric amounts, and with Bub3-BubR1 fully

incorporated to Mad2-Cdc20, more effectively inhibit APC/C-Cdc20co-activator complex (Fig.2) (Nilsson et al., 2008).

Figure 2

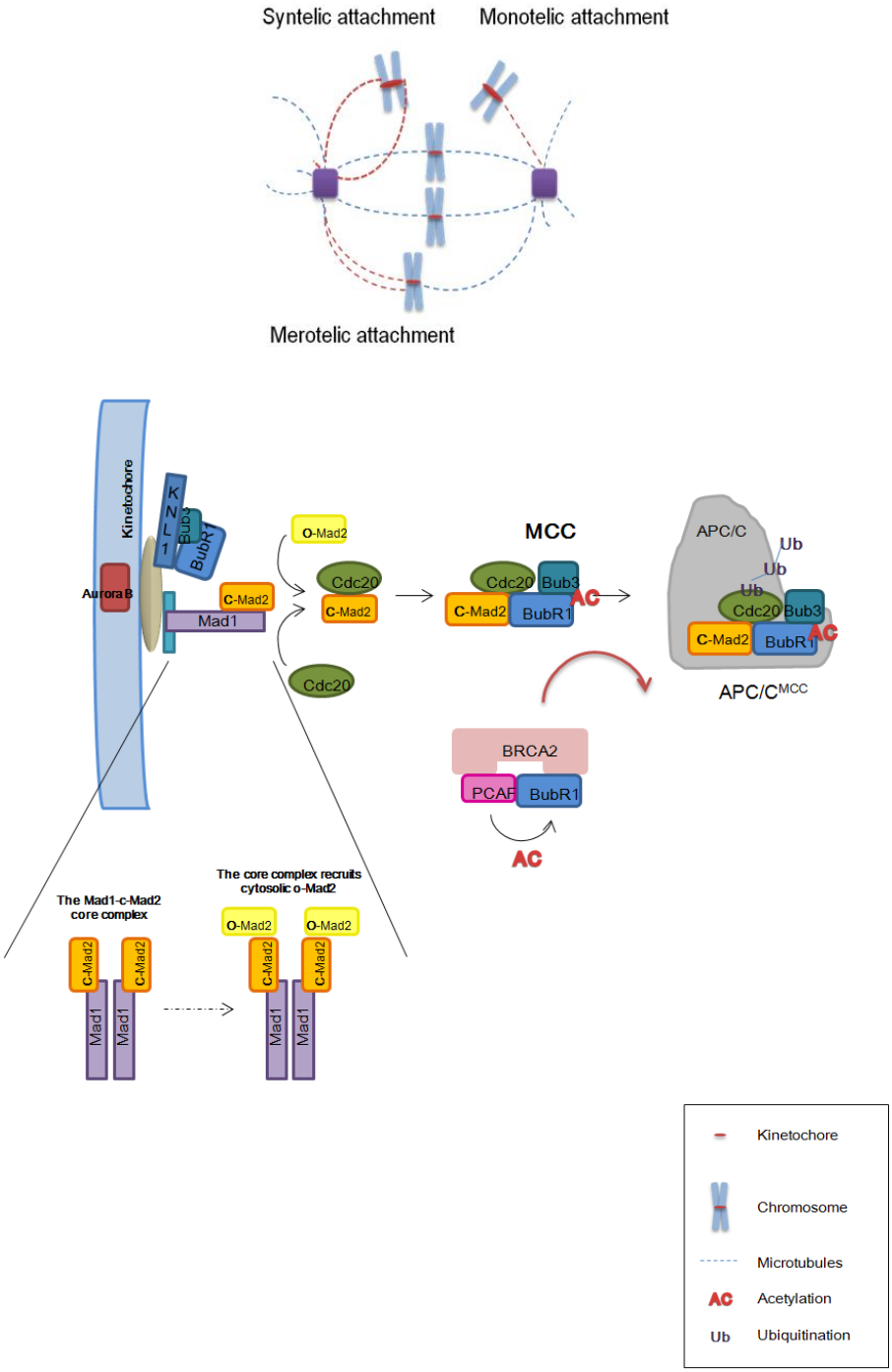
Syntelic attachment
Monotelic attachment
Merotelic attachment
Kinetochore
KNL1
Bub3
BubR1
Aurora B
C-Mad2
Mad1
O-Mad2
Cdc20
MCC
Bub3
AC
APC/C
Ub
APC/C^MCC
BRCA2
PCAF
The Mad1-c-Mad2 core complex
The core complex recruits cytosolic o-Mad2
Kinetochore
Chromosome
Microtubules
Acetylation
Ubiquitination

Fig.2 Activation of SAC

(Top) Mechanical sensor at unattached/tensionless kinetochore is converted to chemical signaling to inhibit APC/C in prometaphase. When the sister kinetochores attach to microtubule spindles emanating from a single spindle pole (syntelic attachment) or when only one of the sister kinetochores attach to the mitotic spindle (monotelic attachment), SAC is activated.

(Bottom) Upon SAC activation, MCC accumulates at the kinetochores in a hierarchical manner. MCC in the cytoplasm binds to APC/C to inhibit the ubiquitination of APC/C substrates. Inhibition of Cyclin B and Securin ubiquitination stops the cell from progressing into anaphase.

I-4. Sensors in SAC

Multiple kinases are involved in the activation of SAC. Mps1 and Aurora B kinase actively recruit checkpoint proteins to kinetochores and sense KT-MT tension, respectively.

Mps1 kinase

Mps1 kinase is recruited to unaligned kinetochores at the autophosphorylated state, and phosphorylates Met-Glu-Leu-Thr (MELT) motifs of KNL1. Activity of Mps1 is important for recruitment of Mad1-c-Mad2 complex and Bub3-BubR1 complex to kinetochores (Funabaki and Wynne, 2013). In yeast, Bub1 recruitment to kinetochores is dependent on the phosphorylation of KNL1 by Mps1, which in turn allows the formation of Bub3-Bub1 or Bub3-BubR1 complexes at kinetochores (Yamagishi et al., 2012; Krenn et al., 2014). In addition, Mps1 also has an important role in regulating Mad2 template mechanism, putting the kinase at the top of the SAC signaling. Mps1 promotes recruitment of the RZZ complex to the kinetochores, which in turn recruits Mad1-c-Mad2. After recruiting the RZZ complex, Mps1 activity is needed to maintain the flow of o-Mad2 to the MAD1-c-MAD2 core complex (Hewitt et al., 2010). Continuous Mps1 activity is important, as inactivation of Mps1 after SAC silencing leads to block the assembly of Mad2-Cdc20 complex, essential to sustaining the SAC (Maciejowski et al., 2010).

Aurora B kinase

Aurora B Ser/Thr kinase has multiple substrates in mitosis, reflecting its broad implications throughout the cell cycle. Aurora B is included in the chromosomal passenger complex (CPC), constituted of INCENP (Inner centromere protein), Survivin and Borealin. At the entry of prometaphase, Aurora B relocates to inner centromere region from the chromosome arms. Aurora B functions in regulating KT-MT attachments and SAC signaling (F.Wang et al., 2012). If erroneous KT-MT attachments are made, such that tension is not generated at sister chromatid kinetochores (through bipolar-attachment), Aurora B destabilizes KT-MT attachment by phosphorylating the KMN network (e.g. Hec1), to lose their attachment to microtubules (Cheeseman et al., 2006; DeLuca et al., 2006). Hence, unattached kinetochores are generated to allow proper KT-MT attachments to reoccur. How concentrated localization of Aurora B at inner centromere during prometaphase relates to phosphorylation of distal targets at outer kinetochores could be explained by the "diffusion-based gradient" model (E.Wang et al., 2011). According to this model, locally concentrated activity of Aurora B at centromere is dependent on the concentration and phosphorylation of the C-terminus of the INCENP. When functional INCENP is vacant at centromeres, Aurora B is then free to reach immobile, distal targets by diffusion in addition to its activation at centromeres (E.Wang

et al., 2011). These phosphorylated substrates are dephosphorylated in metaphase (Welburn et al., 2010), consistent with the localization of PP1 and PP2A phosphatases at kinetochores (Kim et al., 2010).

In addition, independent to the KT-MT attachment regulation, Aurora B also plays a more direct role in SAC signaling (Hauf et al., 2003; Santagueda et al., 2011; F. Wang et al., 2012; Saurin et al., 2011). Several studies have pointed out the implication of Aurora B in SAC signaling. One way is by potentiating SAC signaling at the onset of mitosis by recruiting Mps1 to kinetochores. Upon Aurora B inhibition and deletion of Hec1, Mps1 activation and SAC establishment are delayed and this in turn is rescued by tethering Mps1 to kinetochores (Saurin et al., 2011). Furthermore, analysis with the Haspin inhibitor which targets protein Haspin has provided further insight. Haspin phosphorylateshistone H3 at Thr-3 to provide the docking site for Aurora B complex at kinetochores. When cells are treated with the Haspin inhibitor, phosphorylation of H3T3 decreases, resulting in loss of centromere located Aurora B and phosphorylation of its substrates (F. Wang et al., 2012). In consequence, along with alignment defects in metaphase, SCA signaling is compromised as evident from deterred response to activation by nocodazole and delay in recruitment of BubR1 to kinetochores (F.Wang et al., 2012).

It is clear that major kinases active at the epic of SAC signaling are Aurora B and Mps1, potentially aiding in recruitment of checkpoint proteins to kinetochores at the onset of prometaphase. Considering the fact that SAC is sensitive and checkpoint proteins have fast turnover rates, the nature of the signaling in SAC is likely to be complex and meticulously shaped. Thus, it would be interesting to delve into how post-translational modifications of SAC proteins layer the molecular built up of SAC to aid efficient transmission of the SAC signals throughout the cytoplasm.

I-5. Roles of BubR1 in mitosis

BubR1 is an evolutionarily conserved SAC protein with multiple domains. It is one of the key proteins constituting the MCC, present at unattached kinetochores and cytosol in mitosis. Main regions of BubR1 can be classified into **1)** two N-terminal Lys-Glu-Asn KEN box motifs in vicinity to each other, with putative destruction box (D box) in between, **2)** tetratricopeptide repeat (TPR) also present at the N-terminus, the interacting region to Blinkin and KNL1 (Kiyomitsu et al., 2007; D′arcy et al., 2010), **3)** followed by Gle2-binding sequence (GLEBS) motif mediating binding to Bub3 (Taylor et al., 1998), **4)** internal Cdc20 binding domain, needed for Mad2 independent interaction with Cdc20 (Fiore et al., 2015; Diaz-Martinez et al., 2015), **5)** and lastly, carboxyl terminal ‘kinase’ domain (Kapanidou, M. et al., 2015) (Fig.3).

Functional units of BubR1

The KEN box of BubR1 is crucial for SAC function. KEN boxes can act as degrons of APC/C (Pfleger and Kirchner, 2000). Indeed, study with budding yeast homolog MAD3 has shown that MAD3 acts as a pseudo substrate, competing with real substrate Hsl1 for Cdc20 binding within the APC/C (Burton and Solomon, 2007). In detail, the mechanism was elucidated on how the first and second KEN boxes cooperate in human

BubR1, to block substrates to the APC/C-Cdc20. In mitotic cells, the N-terminus of BubR1 including the first KEN box is necessary and sufficient to assembling with Cdc20, Mad2 and APC/C (Lara-Gonzalez et al., 2011; Malureanu et al., 2009). Deletion of the second KEN box is negligible in forming BubR1-MCC complex, yet both KEN1 and KEN2 boxes are needed for SAC activity. When Lys-Glu-Asn in each KEN Box is mutated to degenerate Ala-Ala-Ala (AAA form), cells expressing such mutants fail to be arrested in mitosis compared to cells expressing wild type BubR1 (Lara-Gonzalez et al., 2011). How KEN2 box affects the SAC activity is explained by measuring APC/C ubiquitination activity with BubR1 KEN box mutants assembled into the MCC bound APC/C complex (APC/C-MCC). Interestingly, when BubR1 with mutated KEN2 box is incorporated into the APC/C-MCC, the ability of APC/C to degrade its substrate Cyclin B is enhanced compared to the APC/C-MCC in which either KEN1 mutated BubR1 or wild type BubR1 is incorporated (Lara-Gonzalez et al., 2011). Furthermore, mutation in the KEN2 box hinders recruitment of the substrate (Securin) to the APC/C-MCC (Lara-Gonzalez et al., 2011). Yeast cryo-EM structure analysis on MCC supports the idea that MAD3 (equivalent to N-terminus of human BubR1) induces displacement of Cdc20 from the bi-partite receptor (Chao et al., 2012). Thus, KEN-box containing MAD3/ BubR1 acts as a pseudo substrate because it efficiently inhibits APC/C-

Cdc20 activity.

TPR motif of BubR1 is crucial to the kinetochore localization activity of BubR1. This domain allows BubR1 to directly bind to Blinkin and KNL1 at the Met-Glu-Leu-Thr (MELT) motif repeat (Kiyomitsu et al., 2007; D'Arcy et al., 2010). Another region central to the kinetochore localization of BubR1 is the stretch of 40 amino acid residues called the GLEBS motif, needed for specific binding with Bub3 (Larson et al., 2007). Bub3 itself is also recruited to kinetochores by Bub1 upon phosphorylation of KNL1 MELT domain at prometaphase (Primorac,I. et al., 2013). Thus, Bub complexes altogether enhance the kinetochore localization activity of BubR1. This is further confirmed through mutagenesis analysis; BubR1 with mutation at E406K in the GLEBs motif fails to bind to Bub3 and localize to kinetochores (Malureanu et al., 2009).

Middle region of BubR1, following the GLEBs motif is called the internal Cdc20 binding site (IC20BD). This region spans over residues 490-560 and plays an important role in binding to Cdc20, independent of Mad2 (Lischetti et al., 2014). In different studies, this region was also termed at ‘ABBA’ motif referring to its identification in Cyclin A, Bub1, BubR1 and Acm1 (Di Fiore et al., 2015) or the “Phe” box due to the two phenylalanine residues (Diaz-Martinez et al., 2015). This domain is implicated in eliciting SAC response at full strength and recruiting Cdc20 to the kinetochores

during SAC (Di Fiore et al., 2015).

The C-terminus of human BubR1 is the kinase domain (738-1014aa), which is unique to the vertebrate counterpart of BubR1. The requirement for the kinase domain was suggested in proper KT-MT attachments (Huang H. et al., 2008; Mao et al., 2003), but rescue experiments using the kinase dead mutant (K1204A) of BubR1 suggested that the effect of kinase domain on chromosome congression is trivial (Elowe et al., 2007). Moreover, it has been suggested that BubR1 is actually a pseudokinase. Even though the protein possesses the catalytic triad characteristic of conventional kinases, the kinase domain is used only as a structural stabilizer (Suijkerbuijk et al., 2012).

Post-translational modifications of BubR1

BubR1 is post-translationally modified in mitosis. Modifications take form in phosphorylation, acetylation, sumolylation and ubiquitination. These post-translational modifications of BubR1 affect the localization, stability, half life and hierarchical order in assembly of checkpoint proteins (Kapanidou, M. et al., 2015).

BubR1 is heavily phosphorylated in mitosis, causing electrophoretic upshit. Hyperphosphorylation of BubR1 has been suggested to affect mitotic progression and mainly, establishment of tension and attachment of

microtubules at kinetochores. The evolutionarily conserved Ser/Thr residues of BubR1 are phosphorylated by Cdk1, Plk1 and Mps1. The threonine at 620 is phosphorylated by Cdk1, and this allows Plk1 to bind to BubR1 via the polo-box-domain. Additionally, serine at 676 is phosphorylated as well by Plk1, specifically at unattached kinetochores, implying its role in KT-MT attachment (Elowe et al., 2007). Another phosphorylation at 670 serine by Cdk1 (possibly also Mps1) is suggested to reflect tension sensitive KT-MT attachments (Huang, H. et al., 2008). Lately, threonine at 680 is suggested to be phosphorylated by Plk1 as well (Suijkerbuijk et al., 2012). Through domain architecture and genetic screening, the domain (647-697aa) which encompasses the previously mentioned phosphorylation sites as well as the novel 680 threonine, is designated as the "KARD (Kinetochore Attachment Regulatory Domain)" domain (Suijkerbuijk et al., 2012; T.Kruse et al., 2013). The KARD domain is strictly regulated by Plk1 phosphorylation and promotes direct interaction of BubR1 with the PP2AB56a phosphatase to counteract excessive Aurora B activity at kinetochores. In parallel, when Plk1 is inhibited or BubR1 is depleted from cells, the level of PP2AB56a diminishes at kinetochores and phosphorylation of Aurora B substrates is elevated (Suijkerbuijk et al., 2012). Collectively, the conserved phosphorylations of BubR1 seem to be primarily involved in mediating KT-MT attachment.

Another post-translational modification which shows high functional relevance in regulating BubR1 in prometaphase is acetylation. In prometaphase, BubR1 is acetylated at the 250th lysine by PCAF acetyl-transferase (Choi et al., 2009). Acetylation of BubR1 at the 250th lysine switches BubR1 from substrate to inhibitor of APC/C. In line of that, mitotic timing is shortened when deacetylated BubR1 is expressed in cells (Choi et al., 2009). The specific acetylation of BubR1 by PCAF occurs at kinetochore, using tumor suppressor BRCA2 as the platform (Choi et al., 2012). Interestingly, when the interaction of BRCA2 and BubR1 is abrogated by ectopically expressing the BubR1 binding C-terminus of BRCA2, the mice spontaneously develop tumors (Choi et al., 2012). Hence, it is plausible that the involvement of tumor suppressor BRCA2 in licensing acetylation of BubR1 suggests a possible role of BubR1 acetylation in tumorigenesis.

Figure 3

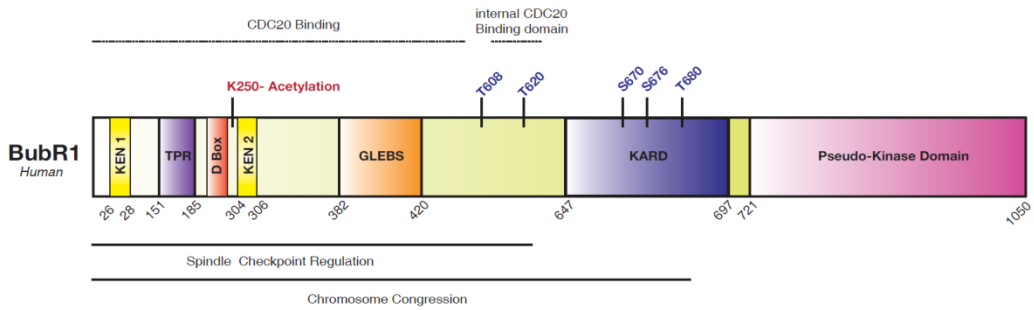

K250- PCAF
T608- autophosphorylation
T620- Cdk1
S670- Cdk1/Mps1
S676- Plk1
T680- Plk1

Fig.3 Regulatory domains and post-translational modifications of human BubR1 protein

Main regions of BubR1 are classified into **1)** two N-terminal Lys-Glu-Asn KEN box motifs with putative destruction box (D box) in between, **2)** tetratricopeptide repeat (TPR), **3)** Gle2-binding sequence (GLEBS) motif, **4)** internal Cdc20 binding domain, and **5)** carboxyl terminal 'kinase' domain. BubR1 is phosphorylated at indicated Ser/Thr by kinases and acetylated at the 250^{th} lysine by PCAF.

I-6. A Novel function of BRCA2 in mitosis

Germ line mutation in tumor suppressor BRCA2 confers susceptibility to tumorigenesis. Functionally, BRCA2 is suggested to play essential roles in preserving chromosome integrity during cell division. BRCA2 deficient cells spontaneously accumulate in aberrant chromosome number and structure. The structural anomalies include breaks at single chromosome or quadriradial and triradial chromosomes (A.Venkitaraman, 2014). Such chromosomal morphology is reflective of defects in homologous DNA recombination (HR) (K.J. Patel et al., 1998). On the other hand, additionally occurring large deletions or translocations reflect inaccurate chromosome segregation (H.Lee et al., 1999). This infers that, in addition to the well established roles of BRCA2 in regulating HR, BRCA2 is also involved in cell division. Indeed, checkpoint activity is intricately related with understanding tumorigenesis in BRCA2 cancer.

The study with murine *BRCA2* deficient MEFs shows that inactivation of cell cycle checkpoints relive growth arrest or apoptosis, initiating neoplastic transformation (H.Lee et al., 1999; Skoulidis, F. et al., 2010). In this line, mutation of *p53* is frequently reported in BRCA2 cancer cells (T.Crook et al., 1998).

Surprisingly, BRCA2 itself is directly related to controlling cell division, one way by achieving it through regulation of SAC. The first implication

was made from observing mutations in *Bub1* and *BubR1* in BRCA2 lymphomas. Also, the fact that Bub1 expression could reverse growth arrest and initiate transformation in BRCA2 MEFs supported the idea (Lee et al., 1999). The later work from Choi, Park and Lee et al. (2012) shows that such aneuploidy found in BRCA2 deficient MEFs arise due to involvement of BRCA2 in control of BubR1 acetylation. In prometaphase, BRCA2 recruits PCAF and mediates association with BubR1 to enforce acetylation of BubR1 at kinetochores (Choi et al, 2009). Furthermore, transgenic mouse model over expressing C-terminal region of BRCA2 (B2-9) which is needed to bind BubR1, spontaneously develop tumors. The B2-9 fragment is located at the far C-terminal end of BRCA2 when BRCA2 is divided into 9 pieces (Esashi et al., 2005). In these mice, mitotic function of BRCA2 in mediating acetylation of BubR1 is disrupted due to competition between B2-9 fragment and endogenous BRCA2 (Choi et al., 2012).

These previous results suggest several questions to be answered. As implied from the spontaneous tumorigenesis from B2-9 mice, does acetylation of BubR1 carry a tumor suppressive role? At molecular basis, BRCA2 brings BubR1 and PCAF together at kinetochores as the platform for BubR1 acetylation (Choi et al., 2012). But how is BRCA2 recruited to kinetochores in mitosis and could it extend its role as a scaffold to support SAC signaling in mitosis?

I-7. SAC silencing

When all KT-MT attachments are satisfied, cells enter anaphase to complete chromosome segregation and eventually exit mitosis. This event requires inactivation of kinases and activation of phosphatases to reverse phosphorylation of kinase targeted substrates and to generate checkpoint silencing signals at kinetochores. At the end point of SAC silencing, MCC disassembles from APC/C (Lara-Gonzalez et al., 2012). The complete nature of signals for SAC silencing and how microtubule binding satisfies SAC are unclear. But possibly, stretches in kinetochore due to pulling forces generated by microtubules could be a cue (Uchida, K. S., 2009). Aurora B undertakes the role of “tension sensor” at kinetochores and its phosphorylation activity leads to destabilization of KT-MT attachment (Funabaki et al., 2013). Hence, to stabilize KT-MT attachment, physical distancing of Aurora B substrates from kinetochores and counteracting Aurora B activity in Plk1 dependent manner are required (Suijkerbuijk et al., 2012; Liu, D. et al., 2012). The plk1 dependent phosphorylation of BubR1 at the KARD domain recruits phosphatase PP2AB56a which counteracts Aurora B activity (Suijkerbuijk et al., 2012). Not only is PP2AB56a required, but also PP1 phosphatase is targeted to kinetochores to dephosphorylate Aurora B substrates and to support stabilization of microtubule attachments (Liu, D et al., 2010).

In eukaryotes, the stable KT-MT attachment strips Mad2 and

Mad1from kinetochores, mediated by the minus end directed motor protein dynein (Howell et al., 2001). The removal of Mad1 and Mad2 from kinetochores is critical, as artificial tethering of Mad1 to kinetochores delays anaphase onset (Maldonado, M. et al., 2011). In addition, RZZ complex which is required for the recruitment of Mad1 and Mad2 (Buffin, E., 2005) is also stripped away from kinetochores (Chan et al., 2009).

Another key step assuring mitotic exit is the inactivation of APC/C inhibitor, which correlates with the disassembly of MCC from APC/C (Lara-Gonzalez et al., 2012). Several mechanisms and factors have been suggested to contribute to the disassembly of MCC from APC/C. Two key proteins required are P31 comet and APC15, a subunit of the APC/C holoenzyme complex. P31 comet, an interactor of Mad2 functions in two ways: 1) first, by binding to c-Mad2 interface of Mad1-c-Mad2 and interfering with catalysis of recruited o-Mad2 at kinetochores (Yang.M et al., 2007; Mussachio et al., 2007), 2) second, by disrupting MCC bound to APC/C through distortion of interaction between Mad2 and BubR1-Cdc20 (Westhorpe et al., 2011; Teichner et al., 2011). APC15 is responsible for the turnover of MCC and Cdc20 bound to APC/C, in response to SAC signaling. When cells are depleted of APC15, the MCCs and ubiquitinated Cdc20 are stabilized to the APC/C, preventing the ubiquitination and degradation of Cyclin B (Mansfeld et al., 2011). MCC disassembly from APC/C is the

ultimate and necessary molecular transition which needs to happen, as subsequent proteolysis of Securin and Cyclin B by active APC/C-Cdc20 will turn off Cdk1 activity. Based on these previous researches, possibly one can deduce that BubR1 is deacetylated when SAC is satisfied as checkpoint signal regresses.

Collectively, following questions could be raised to attention.

1) Whether acetylation of BubR1 is involved in regulation of MCC assembly and regulation of KT-MT attachment,

2) as implied from the previous research, if acetylation of BubR1 is indeed a tumor suppressive mechanism, and lastly,

3) what molecules aid in BubR1 acetylation and deacetylation in mitosis.

II. Materials and Methods

II-1. Genotyping

PCR was used to genotype the adult BubR1 acetylation-deficient mice using genomic DNA extracted from the tail. The genomic DNA from the *in vitro* cultured ES cells and embryos was extracted using the Direct PCR reagent (Viagen Biotech, Inc.). A 3–5μl sample of the genomic DNA was used for the PCR. The primers for BubR1 were as follows:

5′-CCCTCACAAACGCCTACC-3′ (forward) and

5′-CATCTCACCAGCCCAGAAGA-3′(reverse). The primers flank the region adjacent to the lox p, FRT site in the targeted gene. The resulting PCR products were separated on a 1.5% agarose gel. Using the primers indicated, the WT DNA produced a 145-bp PCR product, and the homozygote mutant allele produced a slower migrating 219-bp band.

II-2. Cell culture, drugs and transfection

MEFs were generated from E13.5-14.5 embryos and passage 4 MEFs were used for experiments. MEFs were cultured in high glucose DMEM (16% FBS, 1% penicillin/streptomycin, 55 μM β-Mercaptanol) in a 37℃ humidified chamber with 10% CO_2. HeLa cells were cultured in high glucose DMEM (10% FBS, 1% p/s) at 37℃ with 5% CO_2.

Inducible HeLa-flippase recognition target (FRT) cell lines were generated by cloning HDAC3 into pcDNA5/FRT/TO construct (a gift from J. Pines, Gurdon Institute, Cambridge, UK). The HeLa-FRT/TO cells (a gift from S. Taylor) were cotransfected with the pOG44 and pcDNA5/FRT/TO-HDAC3 construct, and the cells were selected according to the FLIP-in protocol (Invitrogen). 1 μg/ml of doxycycline was treated to induce the ectopically expressing genes.

2.5 mM thymidine was used to block cells in S phase. After 16 hr, cells were washed with PBS twice and released into media. 200 ng/ml nocodazole or 10 μM taxol or 100 μM monastrol and 10 μM MG132 was treated to enrich cells in mitosis.

DNA constructs or siRNA were delivered to cells using lipofectamine 2000 (according to manufactor's protocol) or Neon microporator (Invitrogen) at 1300 mV, 2 ms, 1 pulse.

II-3. Constructs, antibodies and siRNA

PP2A-B56a-expressing constructs were gifts from G. Kops (University Medical Center, Utrecht, Netherlands). *EGFP-PP2A-B56a* expressing construct was generated by sub cloning *PP2A-B56a* into EGFP-N1 vector (Invitrogen). Various BubR1 constructs were generated by PCR and sub cloned into pcDNA3.1-mcherry for expression in cultured cells. The

K250R/Q, KARD-3A/D and T680A/D BubR1 mutants were generated by site-directed mutagenesis using pcDNA3.1-mcherry BubR1 as the template.

The following antibodies were used: anti-Cyclin A (H-432; Santa Cruz Biotechnology Inc), anti–Cyclin B (H-433; Santa Cruz Biotechnology Inc), anti-Mad2 (C-19; Santa Cruz Biotechnology Inc), anti-PCAF (H369 and E-8; Santa Cruz Biotechnology Inc), anti-Cdc20 (H-175; Santa Cruz Biotechnology Inc), anti-APC3 (H-300; Santa Cruz Biotechnology Inc), anti-HDAC2 (H-54; Santa Cruz Biotechnology Inc), anti–α tubulin (DM1A; Sigma-Aldrich), anti-beta actin (AC-15; Sigma-Aldrich), anti-BubR1(BD), anti-FITC conjugated BrdU (BD), anti–PP2AB56a (BD), anti-CREST (Cortex Biochem), anti-HDAC3 (ab7030; Abcam), anti-Plk1 (ab26-298; Abcam), anti-phosphohistoneH3 (06-570; Millipore), anti-BRCA2 (Ab-1; Millipore), anti-BRCA2 (B2-4 antigen; custom made sheep polyclonal) and Alexa Fluor 657, 568, 488 antibodies (Invitrogen). The anti-Bub3 antibody was a gift from S. Taylor (University of Manchester, Manchester, UK). The anti-Mad2 and anti-Mad1 antibodies were obtained from H. Yu (University of Texas Southwestern Medical Center, Dallas, TX), anti–pS55 Hec1 antibody was obtained from J. Deluca (Colorado State University, Fort Collins, CO).

The following siRNAs were used:

HDAC3 3′UTR: 5′-GAGGACTACATTGACTTCCTGCAGA-3′,

BubR1 3′UTR: 5′-GUC UCA CAG AUU GCU GCC U-3′, BRCA2: 5′-GAA GAA CAA UAU CCU ACU ATT-3′

II-4. Immunoprecipitation (IP) and western blot (WB)

Cells were lysed in NETN buffer (150 mM NaCl, 1 mM EDTA, 20 mM Tris, pH 8.0, and 0.5% NP-40) supplemented with protease inhibitors for IP and WB analysis. Cells were incubated on ice for 20 min and supernatants were collected after centrifugation at 4℃, 12000 rpm. Cell lysates were precleared for 1 hr at 4℃ with protein A/G beads and subjected to immunoprecipitation with indicated antibodies at 4℃ o/n. Immune-complexes were precipitated by incubating with A/G beads for 2 hr. Before elution with 3x SDS sample buffer, immunoprecipitated beads were washed 3 times with the lysis buffer.

II-5. Immunofluorescence assay (IFA)

Cells were grown on cover slips, fixed in 4% paraformaldehyde in PBS, and permeabilized by incubation in 0.5% Triton X-100 in PBS (0.5% PBST) for 20 min at RT. 3% BSA in 0.1% PBST was used as a blocking agent and antibody dilution solution. After blocking for 1 hr at RT, cells were incubated with the indicated primary antibodies for 1 hr at RT or overnight at 4℃ followed by incubation with fluorescence-conjugated secondary antibodies. DNA was detected using DAPI and cells were mounted in vectashield (Vector laboratories).

II-6. Chromosome spreads

For the SKY analysis, the *K243R/+*MEFs (at passage 27) were treated with 5 μg/ml colcemid for 7 hr before fixation. The SKY analysis was performed at the Molecular Cytogenetics Core at the University of Texas M.D. Anderson Cancer Center.

For chromosome spreads coupled with immunofluorescence assays, cells were incubated with 200 ng/ml nocodazole for 4 hr. To harvest cells, media was removed and cells were washed with PBS, and then pelleted. Cells were swelled in 0.2% KCl and 0.2% trisodium carbonate containing water and cytospinned at 850 rpm for 5 min. The slides were subjected to immunofluorescence assay as described.

II-7. Histopathology

Tissue specimens were collected from all organs that exhibited an abnormal appearance. Hematoxylin and eosin (H&E) staining was conducted following the standard procedures. First, paraffinized tissue block was deparaffinizationin xylene, followed by rehydration in ethanol in a serial manner (100%, 95%, and 70%), and subjected to hematoxylin staining. Then the specimen was decolorized in acid alcohol and counterstained with eosin. H&E or immuno histochemical stains and were reviewed by the pathologist.

II-8. Microscope image acquisition and processing

Fixed cell images were acquired with a microscope (Delta Vision; Applied Precision) equipped with a 100× objective lens (Olympus). The images were obtained with 0.2-μm-distanced optical sections in z-axis. Each section was deconvoluted and projected into one image using the softWoRx software (Applied Precision) for image display.

For live-cell imaging, cells were monitored using the UPlanFLN 40×/NA 1.30 oil lens on a microscope (DeltaVision; GE Healthcare) equipped with a charge-coupled device camera (Photometrics) in a CO_2 chamber at 37℃ (Applied Precision). The cells were seeded in a glass-bottom dish containing culture media and images were acquired every 5 min at 7-μm-distanced optical section using a 20× objective lens (Olympus).

II-9. Cold stable microtubule assay and scoring of the immunofluorescence intensity

The cells were treated with 10 μM MG132 for 2 hr and incubated with serum-free DMEM containing 20 mM Hepes, pH 7.3, for 10 min on ice. When cold MT assay was performed to assess recovery from monastrol treatment, cells were treated with 100 μM monastrol for 3 hr. In the final hour, cells were incubated with 10 μM MG132 as well. Monastrol-arrested cells were washed at least three times with fresh media containing 10 μM MG132. The cells were released into media with 10 μM MG132 for 1 hr.

The cells were fixed in 4% paraformaldehyde for 10 min and the immunofluorescence assays were performed as needed. Images were acquired and processed using DetaVision Softworx software (GE Healthcare), and the images for display were generated by projecting the sum of the optical sections. Quantitative analysis of the immunofluorescence was performed in the projected images using the Image J software (National Institutes of Health). For quantification of intensities at kinetochores, a mask covering each kinetochore foci was created within a circular region, and the mean pixel intensities were obtained. More than 300 kinetochores were scored for the intensities in each experiment for statistical analysis.

II-10. Cell cycle analysis

Three independent experiments were conducted using early passage MEFs. MEFs were serum starved with 0.1% FBS for 72 hr and forced to enter the cell cycle after stimulation with 20% FBS. 8 x10^4 MEFs were seeded onto cover slips and pulsed with 10 μM BrdU at indicated time points before fixation with cold Methanol (-20℃). BrdU positive cells were stained with DAPI and BrdU-FITC antibody for IFA.

∗***K243R/+*** **mice is deposited to Jackson laboratory (Symbol: *Bub1b*** $^{+m1.1Hsl}$**)**

III. Results

BUBR1 ACETYLATION IS REQUIRED FOR KINETOCHORE-MICROTUBULE ATTACHMENT AND STABLE MITOTIC CHECKPOINT COMPLEX FORMATION

III-1. Loss of BubR1 acetylation leads to spontaneous tumorigenesis in mice

SAC is an elaborate safeguard mechanism ensuring equal distribution of genomic contents into daughter cells during mitosis (Mussachio et al., 2007). Constant attachments and detachments are made between microtubules stemming from spindle poles and sister chromatid kinetochores. The forces generated by microtubule dynamics power chromosome movement towards the center. During this course, erroneous attachments could be made and corrected only if SAC is activated at an instant. Thus, the kinetochore which is composed of over 100 proteins is at the center of SAC activation, modulating the stability of KT-MT attachments and relaying the microtubule binding status to SAC (Foley and Kapoor, 2013).

Only one unattached kinetochore is enough to instigate SAC (Rieder et al., 1995). At unattached kinetochores, checkpoint proteins are recruited in a hierarchical manner and propel formation of MCC to inhibit APC/C (Mussachio et al., 2007; Lara-Gonzalez et al., 2011). When APC/C is

inhibited, the degradation of Securin and Cyclin B is blocked, which in turn inhibits progression into anaphase.

BubR1 is a checkpoint protein, constituting the MCC and localizes to kinetochore in prometaphase when SAC is activated (Hardwick et al., 2000; Sudakin et al., 2001). At kinetochores, BubR1 binds to KNL1 and Blinkin, constituting the KMN complex, which is the direct interface of KT-MT attachment (Kiyomitsu et al., 2007; D'Arcy et al., 2010). Furthermore, Plk1 phosphorylation of BubR1 at conserved Ser/Thr residues endows BubR1 a role in docking PP2AB56a phosphatase to the outer kinetochore (Suijkerbuijk et al., 2012; T.Kruse et al., 2013). This recruitment of PP2AB56a counterbalances the phosphorylating activity of Aurora B on the KMN network, stabilizing KT-MT attachments. Therefore, in addition to SAC activity, BubR1 function is crucial in chromosome congression, the bipolar spindle attachment that forms the metaphase plate.

During mitosis, BubR1 is acetylated at 250^{th} lysine by PCAF acetyltransferase, mediated by tumorsuppressor BRCA2. The acetylation of BubR1 could act as a molecular switch, converting BubR1 from substrate to the inhibitor of APC/C upon SAC activation (Choi et al., 2009). Interaction with BRCA2 is necessary for acetylation of BubR1, as BubR1 and PCAF is brought in vicinity by binding to BRCA2 at the C-terminus and N-terminus respectively (Choi et al., 2012). When endogenous BRCA2 and BubR1

interaction is disrupted *in vivo* by over-expressing the BRCA2 C-terminus needed for BubR1 interaction, SAC activity is weakened and mice spontaneously develop tumors (mostly carcinoma and lymphoma) (Choi et al., 2012). As BubR1 acetylation is hampered in these mice, this observation suggests possible tumor suppressive role of BubR1 acetylation.

To further investigate the physiological role of bubR1 acetylation, acetylation defective knock-in mice with the substitution mutant of the conserved 243th lysine with argentine was generated. When mice with heterozygous acetylation deficient allele (*K243R/+*) were intercrossed, mice were born normally at mendelian ratio. The *K243R/+* mice grew without any developmental defects; no aging phenotypes were detected, which were observed in *BubR1*$^{H/H}$ mice (Baker et al., 2004). Also, BubR1 expression and the overall protein level were unaltered in the thymus and testis of the *K243R/+* mice (data not shown). However, out of the 339 mice monitored, no pups with homozygous acetylation deficient allele (*K243R/K243R*) were born (Table.1).

To determine when homozygous mice die, 20 embryo from *K243R/+; K243R/+* intercross were subjected to *in vitro* culture after E.3.5. Four embryos which correlated with the number of homozygous born, died after 3 days of culture, at E6.5. Early death during embryogenesis was due to apoptotic cell death, confirmed with TUNNEL assay (data not shown). This

implies that complete loss of BubR1 acetylation in homozygous accumulate to severely weakened mitotic checkpoint activity during embryogenesis, which cannot be tolerated until birth.

On the contrary, ~30% of *K243R/+* mice were susceptible to spontaneous tumorigenesis at various tissues after a year (Fig.4). When the tumors were analyzed, a significant increase of malignant tumor development in solid and hematologic origin was detected in *K243R/+* compared to WT (Table.2). Also splenomegaly was detected in *K243R/+*, some of which were B cell lymphomas showing white cell expansion as well as high B220 positivity.

Table 1

Genotype	*+/+ : K243R/+*	*K243R/+ : K243R/+*
+/+	29 (63%)	99 (29%)
K243R/+	17 (37%)	240 (71%)
K243R/K243R	0 (0%)	0 (0%)
Total	46	339

Table.1 *K243R/+* mice are born at mendelian ratio

Summary of the crosses and progeny. The *K243R/+* heterozygous mice were intercrossed, and the newborn pups were scored. Total number of mice genotyped and categorized: n=385.

Figure 4

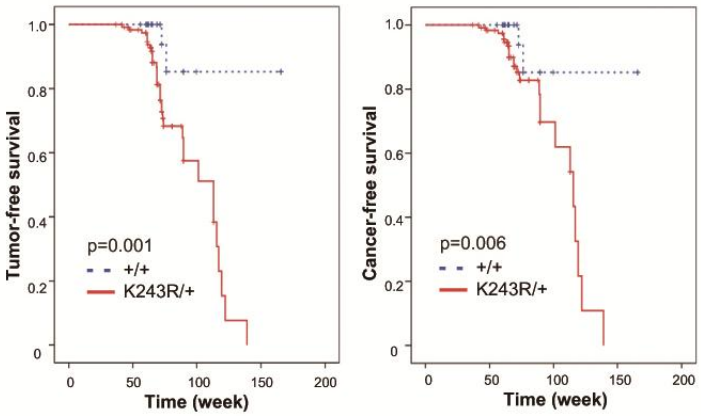
Tumor-free survival
1.0
0.8
0.6
0.4
0.2
0
p=0.001
+/+
K243R/+
0
50
100
150
200
Time (week)
Cancer-free survival
1.0
0.8
0.6
0.4
0.2
0
p=0.006
+/+
K243R/+
0
50
100
150
200
Time (week)

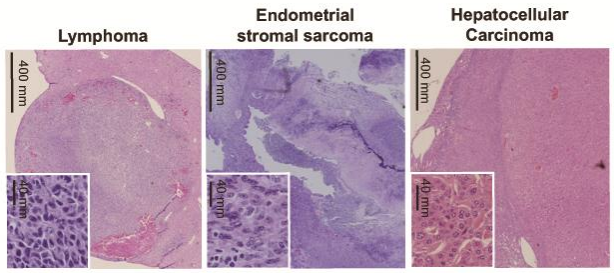
Lymphoma
Endometrial stromal sarcoma
Hepatocellular Carcinoma
400 mm
40 mm

Fig.4 Tumor incidence of *K243R/+* mice

Tumor incidence was assessed using Kaplan-Meier graphs. The tumor-free survival analysis (left) includes both benign and malignant tumors; the cancer-free survival analysis (right) includes only the malignant cancers. Total number of mice analyzed cumulatively: WT, *n*= 41; *K243R/+*, *n*= 121. Representative H&E stained sections of the major pathologies found in the *K243R/+* mice are shown. The insets show high-magnification images.

Table 2

Tumor	*BubR1*$^{K243R/+}$ (n=121)	*BubR1*$^{+/+}$ (n=41)
Malignant tumors	28 (23.1%)	2 (4.8%)
Malignant solid tumors	13 (10.7%)	1 (2.4%)
Hepatocellular carcinoma	6 (5.0%)	
Sarcoma	4 (3.3%)	1 (2.4%)
Adenocarcinoma	2 (1.7%)	
Other cancer	1 (0.8%)	
Hematologic malignancies	15 (12.4%)	1 (2.4%)
Megakaryocyte leukemia	1 (0.8%)	
B cell lymphoma	11 (9.1%)	1 (2.4%)
Metastatic lymphoma/ leukemia	3 (2.5%)	
Benign Tumors	18 (14.9%)	
Total tumor incidence	46 (38.0%)	2 (4.8%)

Table.2 Tumor spectrum of *K243R/+* mice.

Tumor spectrum and analysis are summarized in a table. Mice were monitored until 38 months of age. In *K243R/+* mice, a marked increase in malignant tumor development (23.1%, n= 28) was observed for both solid (10.7%, n= 13) and hematologic (12.4%, n= 15) tumors. Solid tumors and hematologic tumors are further classified into specific tumor types in the table. Benign tumors in *K243R/+* (n= 18) included simple cysts in the genital tract (n= 10), hemangioma (n= 5), epidermal cyst (n= 1), acrochordon (n= 1), and mesenchymal fibroma (n= 1). In WT or *BubR1*$^{+/+}$ mice, 2 cases of tumors in total were detected. Both were malignant tumors, one of which was sarcoma and another, B cell lymphoma.

III-2. CIN in BubR1 acetylation deficient mice

The effect of BubR1 acetylation deficiency at cellular level was more profound. When chromosome content was analyzed by conducting chromosome spreads in MEFs at passage 4, the degree of polyploidy was comparable to that of WT in *K243R/+* MEFs but strikingly, 67% of *K243R/+* MEFs were aneuploid (Fig.5 top). The degree of premature sister chromatid separation (PMSC) was measured as well and *K243R/+* MEFs exhibited a 5.5 fold increase compared to WT (data not shown). PMSC is a hallmark of defective mitotic checkpoint (Basu.J et al., 1999) and could also possibly arise from failure in maintaining sister chromatid cohesion (Hoque et al., 2002; Minshull et al., 1996). Addition of MG132 prior to the fixation of cells for chromosome spreads restored the degree of PMSC in *K243R/+* MEFs to the level comparable to that of WT (data not shown). As treating MG132 interferes with the destruction of Securin and Cyclin B, it could be inferred that PMSC caused by acetylation deficiency in *K243R/+* MEFs is responsive to premature activation of APC/C.

When late passage MEFs were subjected to spectral karyotyping (SKY) analysis, aneuploidy as well as structural chromosome aberrations were detected. Out of 14 samples analyzed, 9 samples had irregular chromosome content. Specifically, one sample harbored chromosome translocation and another sample showed signs of chromosome pulverization, in which

chromosomes were shattered into pieces (Fig.5 bottom). In addition, over 50% of lymphomas also showed aneuploidy and PMSC (data not shown).

It can be inferred that acetylation deficiency of BubR1 not only triggers aneuploidy but also chromosome structural aberrations. Thus CIN is manifested in various forms in *K243R/+*.

Figure 5

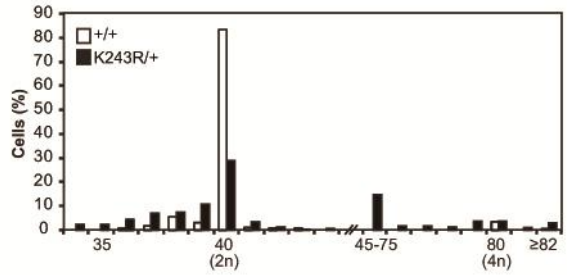

Number of chromosomes per cell

Genotype	Metaphase counted	% diploid (2N=40)	% aneuploid (loss/gain)	% polyploid (4N=80)
+/+	172	83	14 (11/3)	3
K243R/+	610	29	67 (34/33)	4

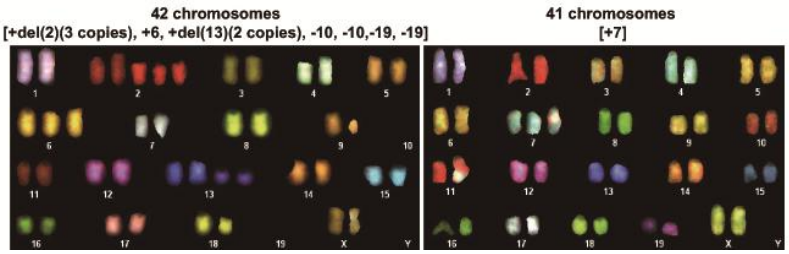

Fig.5 *K243R/+* MEFs are aneuploid and CIN is manifested in various forms at late passage

(Top) The percentage of cells with indicated numbers of chromosomes are shown in the histogram. The results are from three and five different WT and *K243R/+* MEFs, respectively. The table summarizes the analysis of the chromosome numbers in the histogram

(Bottom) Two examples of SKY analysis of the *K243R/+* MEFs cultured for 27 passages are shown (with E.Choi).

III-3. SAC is weakened in BubR1 acetylation deficient mice

The previous study from Choi et al (2009) addressed the implications of BubR1 acetylation in SAC regulation. To understand the molecular basis underlying CIN in *K243R/+* MEFs, progression in mitosis was monitored by time lapse microscopy. *K243R/+* was intercrossed to H2B-GFP expressing transgenic mice. The duration of mitosis was determined by measuring the start of nuclear envelope breakdown (NEBD) to the entry into anaphase, in which chromosomes separate apart. In normal conditions, mitotic timing was shortened on average of 5 minutes in *K243R/+*; GFP-H2B compared to WT; GFP-H2B control. When MEFs were challenged with microtubule depolymerizing drug- nocodazole - or stabilizing drug- taxol-to activate SAC, *K243R/+* MEFs showed a weakened response, escaping mitosis earlier than the control (Fig.6 bottom). Shortened mitotic timing and lowered response to SAC activating drugs suggest that SAC activity is hampered in *K243R/+* MEFs. In addition, as shown in captured images from the live imaging of representative cells (Fig.6 top), chromosomes misaligned and chromosome bridges and lagging chromosomes were shown in 85% of *K243R/+* MEFs.

Figure 6

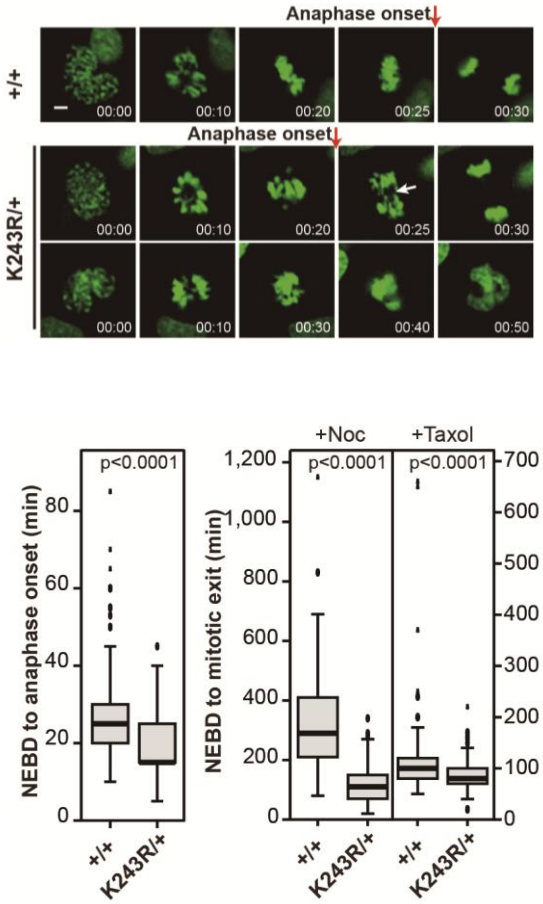
Anaphase onset
+/+
00:00
00:10
00:20
00:25
00:30
Anaphase onset
K243R/+
00:00
00:10
00:20
00:25
00:30
00:00
00:10
00:30
00:40
00:50
NEBD to anaphase onset (min)
p<0.0001
0
20
40
60
80
+/+
K243R/+
NEBD to mitotic exit (min)
+Noc
+Taxol
p<0.0001
p<0.0001
0
200
400
600
800
1,000
1,200
0
100
200
300
400
500
600
700
+/+
K243R/+
+/+
K243R/+

Fig.6 Weakened SAC in *K243R/+* MEFs

Statistical mitotic timing from the NEBD to anaphase onset. The MEFs were subjected to time-lapse microscopy with or without treatment with 200 ng/ml nocodazole or 2 μM taxol. Images were captured every 5 min, and the live images were processed for 36 hr. Without a spindle poison, mitosis required an average of 25 min in the WT cells (*n*= 170) and 20 min in the *K243R/+* MEFs (*n*= 153).After spindle poison exposure, the WT cells remained in mitosis for 331 min with nocodazole (*n*= 66) and 106 min with taxol (*n*= 218). The *K243R/+* MEFs exited mitosis (chromosome decondensation) within 117 min with nocodazole treatment (*n*= 144) and within 87 min with taxol treatment (*n*= 191). The bars in the box represent the median values. The outliers (open circles) and suspected outliers (asterisks), as determined by statistical analysis, are marked (with E.Choi).

III-4. Intact initialization of SAC in BubR1 acetylation deficient mice

I thought the problem of weakened SAC could be scrutinized into either problems in initiation or maintenance of SAC. First to access the initiation step in SAC, the localization of Mad1 and Mad2 at unattached kinetochores was accessed in *K243R/+* MEFs. Prometaphase cells were analyzed at untreated or nocodazole/taxol treated conditions. Nocodazole was treated at high concentration (3.3 μM) in which SAC satisfaction is virtually impossible due to complete depolymerization of microtubules (Yang et al., 2009; Santaguida et al., 2010).As expected, Mad2 was recruited to kinetochores at a higher extent in the nocodazole treated condition compared to the taxol treated condition in general. The degree of Mad2 recruitment to kinetochores was similar between WT, *K243R/+* and haplo-insufficient *BubR1*$^{+/-}$ MEFs. Mad1 was also recruited at a similar degree in all genotypes. The "Mad2 template" model which represents the mode of signal generation during SAC activation includes catalysis of active c-Mad2 from o-Mad2 recruited to Mad1-c-Mad2 positioned at outer kinetochores (De-antoni et al., 2005). No difference in the recruited level of Mad1 and Mad2 compared to WT suggests that signal generation at kinetochores in the initial step of SAC activation is intact in *K243R/+* MEFs (Fig.7).

Figure 7

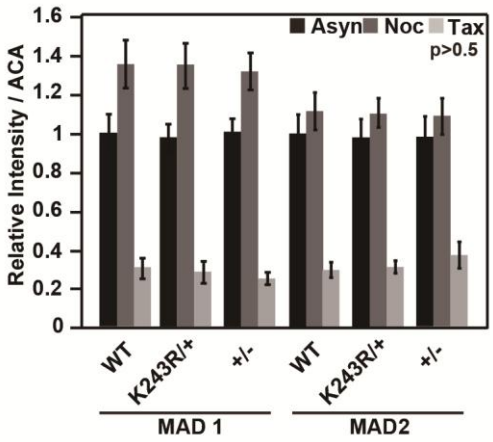

Fig.7 Recruited levels of Mad1 and Mad2 in *K243R/+* MEFs

WT, *K243R/+*, and *BubR1*$^{+/-}$ MEFs were treated with 3.3 μM nocodazole or 2 μM taxol or left untreated. Cells were subjected to co-immunostaining with anti-Mad2 or -Mad1 antibody and FITC-conjugated anti–α tubulin antibodies. 10 unaligned/unattached kinetochores were analyzed per cell. The result is from three independent experiments of 35 different cells each. Relative value compared with the untreated prometaphase cell (Asyn) in WT is depicted by bar graphs (mean ± SEM; $n > 350$ KTs each).

Figure 8

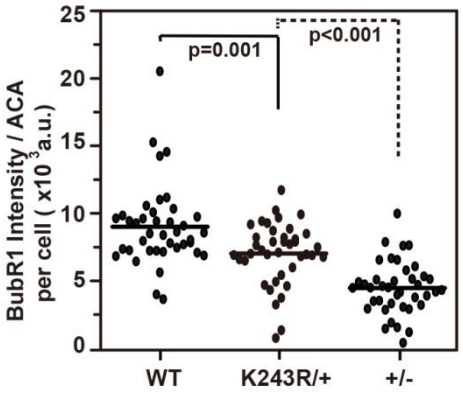

Fig.8 Recruited levels of BubR1 at kinetochores in *K243R/+* MEFs

Quantification of BubR1 at kinetochoress in chromosome spreads after treatment with 200 ng/ml nocodazole. The level of BubR1, determined by anti-BubR1 immunofluorescence in nocodazole-treated prometaphase MEFs, was scored in WT, *BubR1*$^{+/-}$, and *K243R/+* MEFs. Each dot represents the mean BubR1 intensity calculated from 20 randomly picked kinetochoress per cell. 40 chromosome spreads from each genotype were scored in two independent experiments. Mean value is indicated with a line (mean ± SEM; n > 800 kinetochores each).

III-5. BubR1 acetylation deficiency leads to premature mitotic checkpoint complex (MCC) disassembly

In prometaphase, when SAC is active, BubR1 is also recruited to kinetochores along with Mad1 and Mad2 (Musacchio and Salmon, 2007). When the level of BubR1 recruited to kinetochores was accessed in MEFs, the amount of BubR1 recruited to kinetochores was highest in WT MEFs and lowest in *BubR1*$^{+/-}$ MEFs. The level of BubR1 at kinetochores in *K243R/+* MEFs was about 70% of that of WT. As the BubR1 antibody recognizes the deacetylated form of BubR1 as well, one can deduce that the deacetylated K243R-BubR1 is also recruited to kinetochores to fulfill its function in mitosis (Fig.8).

In order to analyze the capacity of *K243R/+* to maintain SAC after activation, the level of MCC was analyzed. Active SAC successfully inhibits APC/C-Cdc20 co-activator complex from ubiquitinating Cyclin B and Securin, to delay the entry into anaphase (Lara-Gonzalez et al., 2012). The MCC, composed of BubR1-Bub3-Mad2-Cdc20, is the potent inhibitor of the APC/C-Cdc20 co-activator complex (Sudakin et al., 2001). The MCC formation in *K243R/+* MEFs was assessed by analyzing the BubR1 immuno-complex in prometaphase (Fig.9b). In nocodazole treated MEFs, the BubR1 level was lower in *K243R/+*, but was restored after treating with the proteasome inhibitor (Noc+MG132). This correlates with the previous

observation that non-acetylated BubR1 is ubiquitinated and targeted for destruction, as a substrate of APC/C (Choi et al., 2009). When the same amount of BubR1 was immunoprecipitaed in the nocodazole treated condition, Cdc20, Bub3 and Mad2 immunoprecipitated from the BubR1 complex were lower than WT control MEFs. The amount of these MCC factors bound to BubR1 was rescued in the MG132 treated condition. Considering that at prometaphase acetylated BubR1 and non-acetylated BubR1 consistently existed in 1:1 ratio in *K243R/+* MEFs (Fig.9a) and K243R-BubR1 did not have a problem in forming MCC (Noc+MG132 panel from Fig.9b), one can deduce the following. After formation of intact MCC upon entry into prometaphase, the presence of K243R-BubR1 in the complex quickly disintegrates Bub3, Mad2 and Cdc20 from APC/C and ultimately leads to failure in SAC maintenance.

Figure 9

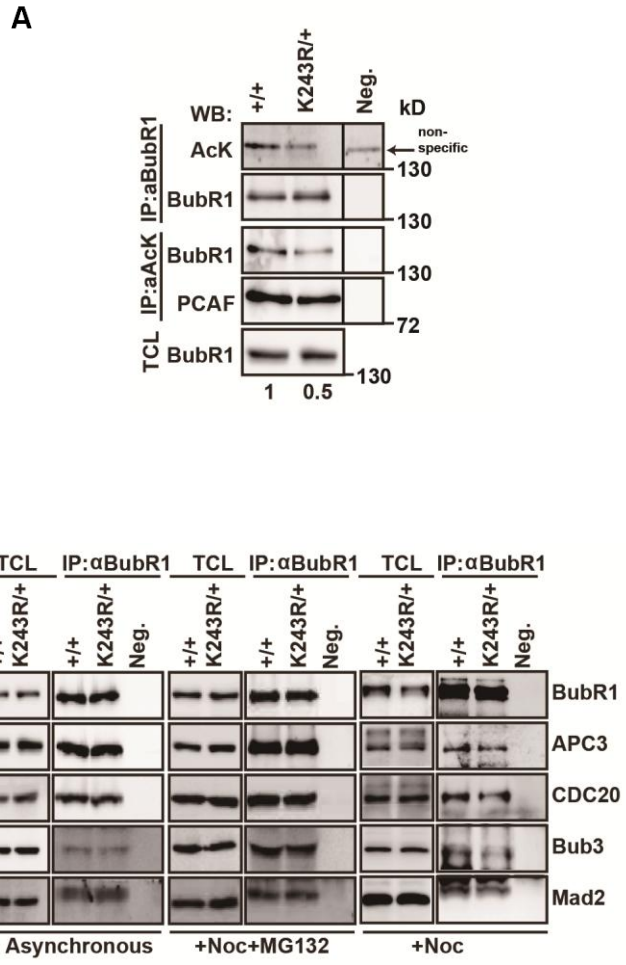
A
WB:
+/+
K243R/+
Neg.
kD
non-specific
IP:aBubR1
AcK
130
BubR1
130
IP:aAcK
BubR1
130
PCAF
72
TCL
BubR1
130
1
0.5
B
TCL
IP:αBubR1
TCL
IP:αBubR1
TCL
IP:αBubR1
+/+
K243R/+
Neg.
kD
130
95
43
34
17
BubR1
APC3
CDC20
Bub3
Mad2
Asynchronous
+Noc+MG132
+Noc

Fig.9 MCC in *K243R/+* MEFs

(A) Assessment of BubR1 acetylation levels in WT and *K243R/+* MEFs. The MEFs were treated with nocodazole (+ MG132) and subjected to IP and WB. The ratio of AcK243/total BubR1, when the level in +/+ cells is normalized to 1, was the same for both the anti-BubR1 and anti-AcK IPs and is marked below each lane. IP with a mixture of rabbit serum and 12CA5 anti-HA antibody is shown as a negative control (Neg). Only a non-specific band migrating just below the band recognized by anti-AcK antibody (top left two lanes) was detected. Black lines in the top four panels indicate the removal of an intervening lane for presentation purposes (with E.Choi).

(B) The asynchronous and mitotic MEFs of WT and *K243R/+*, respectively, were subjected to IP and WB as indicated. For the mitotic extracts, the cells were serum starved for 26 hr, released for 20 hr, and treated with nocodazole for 7 hr. In Noc+MG132-treated MEFs, nocodazole treatment was followed by MG132 treatment for 2 hr before lysis. IP with anti-HA antibody was included as a negative control (Neg.). A sample representing 3% of the total cell lysate (TCL) was loaded as a control (with Haeock Lee).

III-6. BubR1 acetylation deficiency leads to abrupt kinetochore-microtubule attachment

As shown previously, *K243R/+* MEFs harbored CIN manifested in various forms (Fig.5) and high incidence of lagging chromosomes and chromosome bridges occurred in mitosis (Fig.6). Chromosome mis-segregations could arise from lack of attachment to mitotic spindles or inability of chromosomes to bi-orient after the attachments (E.A Foley and Kapoor, 2013). Presence of BubR1 at kinetochores is important for KT-MT attachment. When BubR1 is absent from kinetochores, stable KT-MT attachments are not made (Lampson and Kapoor, 2005). To access whether BubR1 acetylation actively participates in regulation of KT-MT attachment, presence of cold-stable microtubules were assayed. At 4℃, kinetochore microtubules are preferentially stabilized in metaphase cells (Rieder et al., 1981). As MG132 treatment was included in this assay, cells passing through metaphase were collected due to the block in degradation of Cyclin B and Securin. Also degradation of K243R-BubR1 was blocked, enabling localization of both K243R-BubR1 and WT BubR1 to kinetochores. Compared to WT MEFs, *K243R/+* MEFs displayed severe defects in KT-MT attachment. The severity in KT-MT attachment was more profound in *K243R/+* MEFs compared to *BubR1*$^{+/-}$ MEFs, which recruited less BubR1 at kinetochores (Fig.10). Hence, BubR1 acetylation is required for chromosome

congression.

In *K243R/+* MEFs, additional to the kinetochores with cold-stable microtubules, there were also kinetochores with no microtubules attached and some sister chromatid kinetochores were attached to microtubules emanating from single pole only (monotelic attachment) (Fig.10). At kinetochores, erroneous attachment and the resulting lack of tension are sensed by Aurora B ser/Thr kinase located at the inner centromere (F.Wang et al., 2012). When erroneous attachments are made, Aurora B destabilizes KT-MT attachment by phosphorylating the KMN network (e.g. Hec1), to disrupt the KT-MT attachments made (Cheeseman et al., 2006; DeLuca et al., 2006). This generation of unattached kinetochores allows proper KT-MT attachment to reoccur. To test if Aurora B activity is involved in the regulation of KT-MT attachments in *K243R/+* MEFs, two approaches were taken. First, activity of Aurora B kinase was measured by phosphorylation of its substrates at kinetochore and secondly, efficiency of Aurora B mediated error-correction was tested with monastrol washout assay.

Figure 10

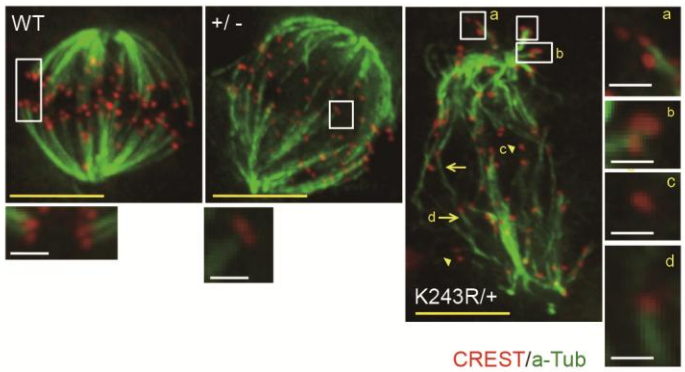
WT
+/ -
a
b
c
d
K243R/+
CREST/a-Tub

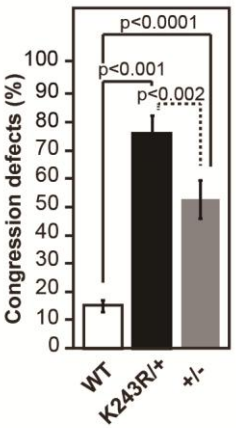
p<0.0001
p<0.001
p<0.002
Congression defects (%)
100
90
80
70
60
50
40
30
20
10
0
WT
K243R/+
+/-

Fig.10 Chromosome alignment defects in *K243R/+* MEFs

WT, *BubR1*$^{+/-}$, and *K243R/+* MEFs were treated with MG132 for 2 hr and subjected to cold microtubule assay, followed by staining with anti–a-tubulin and CREST. Enlarged images of the insets show the properly attached microtubules in WT MEFs; syntelic attachment in *BubR1*$^{+/-}$ MEFs; and unattached (c), syntelic (a and b), and monotelic attachment (d) in *K243R/+* MEFs. Green, α-tubulin; red, CREST immunostaining. Bars: (yellow) 5 μm; (white) 1 μm. The congression defects were scored in cells from each mouse strain in the absence of microtubule poison, and data are shown as bar graphs (mean ± SEM). Number of cells scored: WT, *n*= 75; *K243R/+*, *n*= 102; *BubR1*$^{+/-}$, *n* = 60 (with M.Kwon).

The phosphorylation activity of Aurora B at kinetochores was determined using a phosphorylation specific Hec1 antibody targeting the 55^{th} serine (Deluca et al., 2011). Hec1 is a constituent of KMN network proteins and is a substrate of the Aurora B kinase at kinetochores. After MG132 treatment for two hours, MEFs were subjected to cold microtubule assay and phosphorylation of Hec1 at kinetochores was calculated by measuring the ratio of phosphor-S55 Hec1 (pHec1) to CREST (anti-kinetochore) (Fig.11). *K243R/+* MEFs displayed a 1.3 fold higher level of pHEC1 than WT and *BubR1*$^{+/-}$ MEFs.

To probe the efficiency of error correction in *K243R/+* MEFs, an established assay which enables accumulation of monopolar cells by reversible chemical inhibition of kinesin-5 (Eg5) with monastrol was used (Mayer et al., 1999). In this "monastrol washout" assay, monastrol treatment leads to high incidence of attachment errors as both sister kinetochores are attached to spindles from mono-pole prior to segregation. Such attachment error becomes corrected as monastrol is removed and pole segregates into two, and spindles become bipolar. This error-correction pathway requires Aurora B mediated destabilization and correction of erroneous attachments (Lampson et al., 2004). Monastrol was washed out and cells were released into media containing MG132. After 40 min, cells were fixed and evaluated on the capacity to align chromosomes. Higher percentage of *K243R/+* MEFs

failed to congress properly after KT-MT error-correction compared to WT or *BubR1*$^{+/-}$ MEFs (Fig.12).

Collectively, high incidence of pHec1 and low KT-MT error correction ability point out that Aurora B activity is not balanced to ensure proper KT-MT attachments in *K243R/+* MEFs.

Figure 11

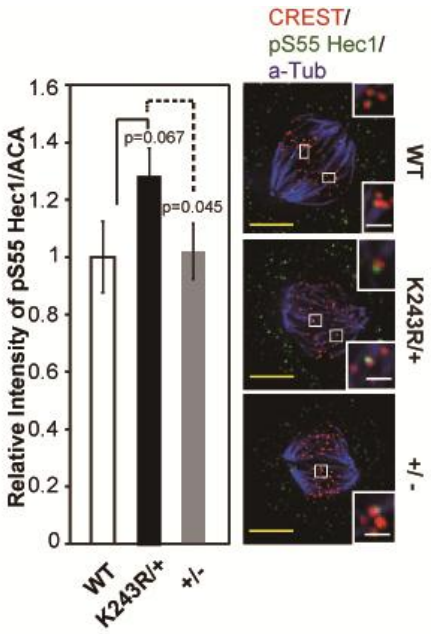

Fig.11 pHec1 intensity at kinetochores in *K243R/+* MEFs

Comparison of phosphorylated Hec1 in metaphase cells. MEFs from WT, *K243R/+*, and *BubR1*$^{+/-}$ mice were treated with 10 μM MG132 for 2 hr and subjected to cold microtubule assay. The levels of pHec1 scored in two independent experiments are shown in bar graphs (mean ± SEM; n > 450 kinetochores; number of cells scored: WT, n= 23; *K243R/+*, n= 34; *BubR1*$^{+/-}$, n= 25). Representative images are shown at the right with enlarged images of individual kinetochores in the insets. Bars: (white) 1 μm; (yellow) 5 μm.

Figure 12

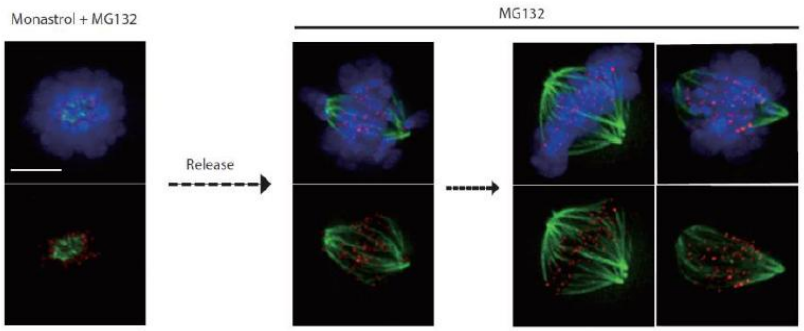
Monastrol + MG132
Release
MG132

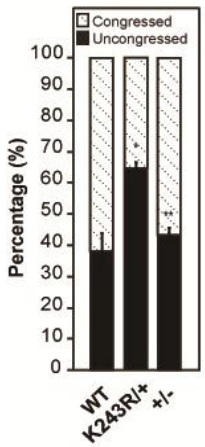
Congressed
Uncongressed
Percentage (%)
100
90
80
70
60
50
40
30
20
10
0
WT
K243R/+
+/-

Fig.12 Recovery of chromosome alignment after monastrol wash out

MEFs were treated with monastrol for 3 hr, washed extensively, and released for an hour in the presence of MG132 and subjected to cold microtubule assay. Congressed and uncongressed chromosomes were scored in two independent experiments and presented in the bar graphs (mean ± SEM; number of cells scored: WT, *n*= 71; *K243R/+*, *n*= 78; *BubR1*$^{+/-}$, *n*= 73). Asterisks mark significant p-values when compared with WT (*, P = 0.1; **, P = 0.5). Yellow bar: 5 μm.

To guarantee stable KT-MT attachment and error correction, Aurora B activity of phosphorylating the KMN network needs to be regulated at a balanced level. Previously, BubR1 has been suggested to bind to PP2AB56a subunit of PP2A phosphatase after phosphorylation at “KARD (Kinetochore attachment regulatory domain)” Domain (Suijkerbuijk et al., 2012; T.Kruse et al., 2013). The phosphorylation of KARD domain is predominantly regulated by Plk1 in prometaphase at kinetochores. The phosphorylated KARD domain serves as the docking site to recruit PP2AB56a, which in turn counteracts Aurora B phosphorylation (Suijkerbuijk et al., 2012; T.Kruse et al., 2013).As hyperphosphorylation of Hec1 in *K243R/+* cells indicated excessive Aurora B activity, the ability of K243R-BubR1 to bind with PP2AB56a was tested. Myc-tagged WT, K250R (acetylation deficient) or K250Q (acetylation mimicking) mutants were ectopically expressed into HeLa-FRT/TO cells expressing PP2AB56a. Immunoprecipitation analysis showed that acetylation deficient BubR1 bound to PP2AB56a at a reduced level of 75% (data not shown). In addition, when EGFP-PP2AB56a was expressed into MEFs, localization of PP2AB56a was reduced to 70% at kinetochores in *K243R/+* MEFs (Fig.13). This was verified with immunostaining of endogenous PP2AB56a with the specific antibody (Fig.14). These results show that BubR1 acetylation is involved in recruitment of PP2AB56a to kinetochores.

Figure 13

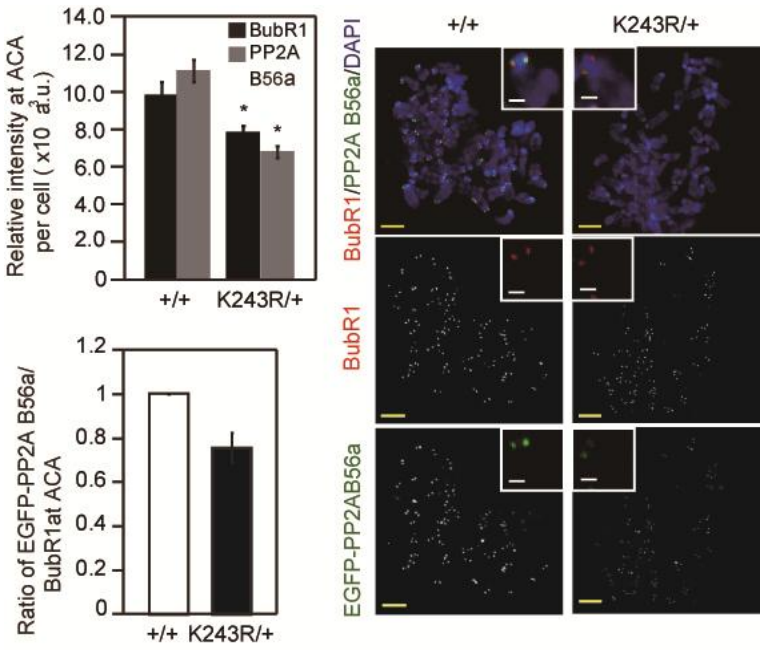
Relative intensity at ACA per cell (x10 a.u.)
BubR1
PP2A B56a
+/+
K243R/+
Ratio of EGFP-PP2A B56a/ BubR1at ACA
+/+
K243R/+
BubR1/PP2A B56a/DAPI
BubR1
EGFP-PP2AB56a

Fig.13 PP2AB56a is recruited at a reduced level to kinetochores in *K243R/+* MEFs

EGFP-PP2A-B56a expressing construct was transfected into *K243R/+* MEFs. 24 hr later, MEFs were treated with 200 ng/ml nocodazole for 4 hr, and then subjected to chromosome spread and immunofluorescence assay. BubR1 was detected by anti-BubR1 antibody and PP2AB56a by the fluorescence of GFP (right). This experiment was done in the absence of MG132. Fluorescence intensity of PP2AB56a relative to BubR1 at kinetochores was scored in WT and *K243R/+* cells and depicted as a histogram (left). The results are from two independent experiments of >600 kinetochores (mean ± SEM; number of cells: WT, *n*= 33; *K243R/+*, *n*= 32; P = 0.061). Red, BubR1; green, PP2A-B56a; blue, DAPI.

Bars: (white) 1 μm; (yellow) 5 μm.

Figure 14

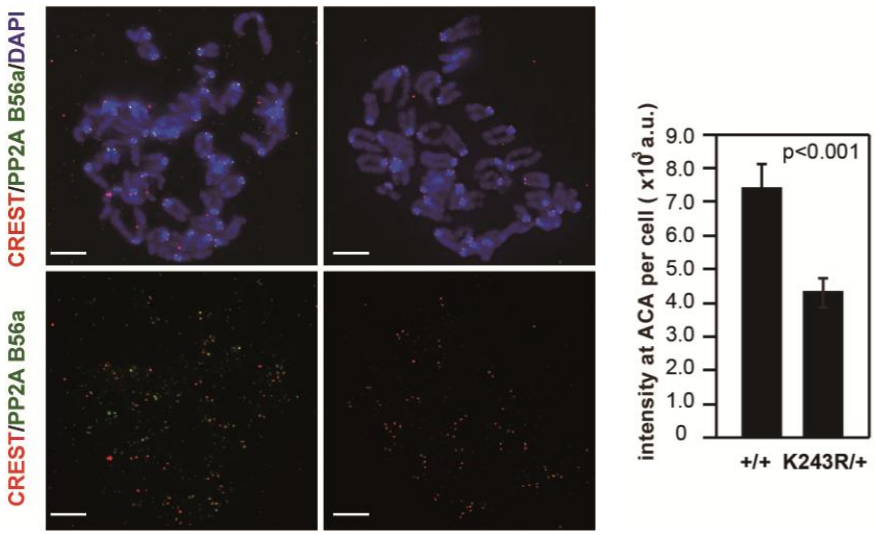
CREST/PP2A B56a/DAPI
CREST/PP2A B56a
intensity at ACA per cell (x10³ a.u.)
9.0
8.0
7.0
6.0
5.0
4.0
3.0
2.0
1.0
0
p<0.001
+/+
K243R/+

Fig.14 The level of endogenous PP2AB56a recruited to kinetochores of*K243R/+* MEFs

PP2AB56a recruitment to kinetochores in WT and *K243R/+* MEFs was analyzed by staining with the antibody specific to PP2AB56a. Metaphase chromosome spreads were coupled with immunofluorescence assay. Immunofluorescence assay was performed with anti-CREST and anti–PP2AB56a. The result is from two independent experiments of 27 cells in each setting (mean ± SEM; $n > 450$ kinetochores). Bars: 5μm.

III-7. Cell cycle profile of cells with acetylation deficiency

Previous mouse models targeting BubR1 are *BubR1*$^{+/-}$ mouse and *BubR1*$^{H/H}$ mouse (Dai et al., 2004; Baker et al., 2004). All three mouse models harbor aneuploidy yet *K243R/+* mouse was the only model which spontaneously developed tumors (Fig.4 and Table.2).

Acetylation of BubR1 is very specific to mitosis (Choi et al., 2009). On the contrary, the two other mouse models have constantly low level of BubR1 expressed throughout the cell cycle, which could possibly affect regulation of BubR1 outside mitosis (Dai et al., 2004; Baker et al., 2004). It has been suggested that BubR1 has a role in interphase, by independently acting as a soluble inhibitor of APC/C-Cdc20 and blocking Cyclin B destruction (Malureanu et al., 2009). When the Cyclin B level was measured throughout the cell cycle in *K243R/+*, it was comparable to that of WT (Fig.15). Also, in mitosis, the acetylation of BubR1 did not affect accumulation of Cyclin B in prophase and mitotic entry (data not shown). In effect, K243R-BubR1 was constantly expressed at the level comparable to WT in various tissues (data not shown). Hence, the protein level or non-mitotic function of BubR1 cannot be a factor affecting the phenotype of *K243R/+* mice.

To compare and verify that acetylation deficiency of BubR1 does not affect other cell cycle phases, the timing of entire cell cycle was analyzed.

First, entry into mitosis was analyzed by synchronizing MEFs into G_o and releasing the MEFs into cell cycle. The entry and exit into specific phases of cell cycle was determined by the rise and fall of Cyclin levels. As fluctuations in Cyclin A and Cyclin B levels were comparable to that of WT, *K243R/+* MEFs did not have a problem in entering mitosis (Fig.15). But the difference in time at the exit of mitosis shown in Fig.6 was not reflected in the fall of Cyclin B level in the western blot (Fig.15) because the cell lysates were harvested at an interval of 2-3 hours. In addition, entry into S phase was analyzed as well by labeling with BrdU. *K243R/+* MEFs did not have a problem entering into S phase as increment in the level of BrdU incorporated was compatible to that of WT MEFs (Fig.16).

Figure 15

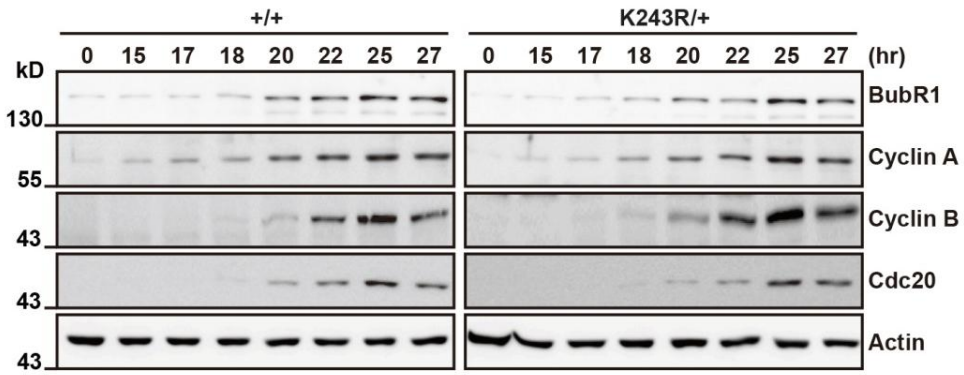

Fig.15 BubR1 acetylation deficiency does not affect entry into mitosis

A comparison on the cell cycle progression in WT and *K243R/+* MEFs. The MEFs were serum starved using 0.1% FBS for 72 hr and forced to enter the S phase after stimulation with 20% FBS. Cell aliquots were collected at the indicated time points and were subjected to western blot using the indicated antibodies.

Figure 16

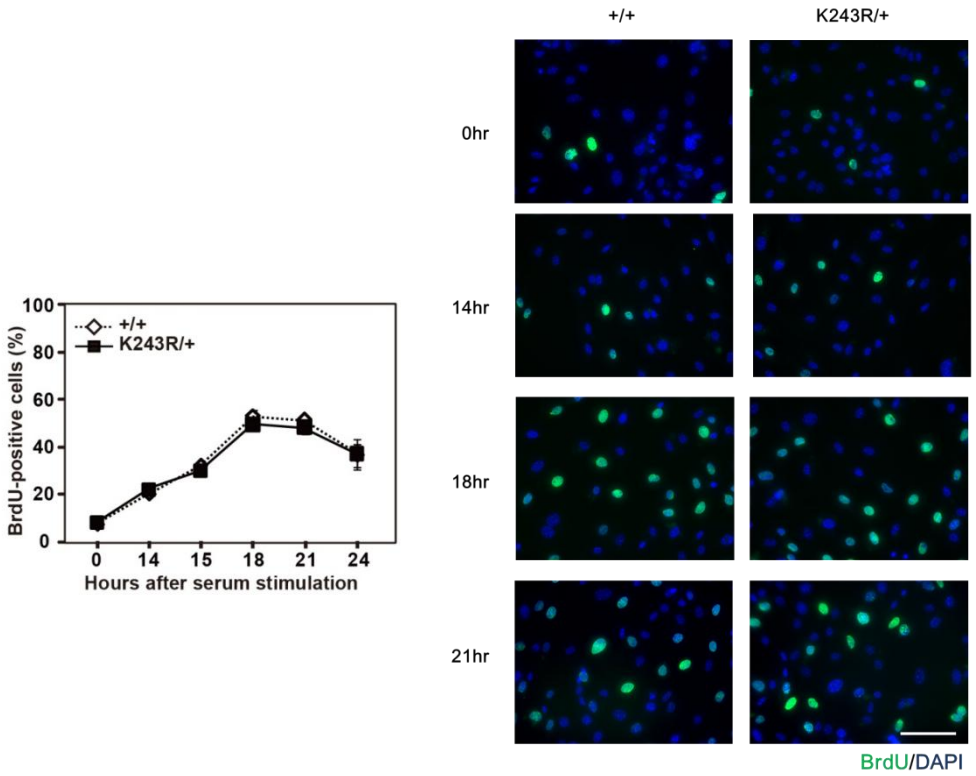
+/+
K243R/+
0hr
14hr
18hr
21hr
BrdU/DAPI
BrdU-positive cells (%)
100
80
60
40
20
0
+/+
K243R/+
0
14
15
18
21
24
Hours after serum stimulation

Fig.16 Duration of S phase in BubR1 acetylation deficient cells

The MEFs were pulsed with BrdU for an hour prior to fixation at the indicated time points after serum stimulation. The results represent the mean of two independent experiments using different siblings. More than 1000 cells were counted at each time point (mean ± SEM). Scale bar: 100μm.

EXTENDED STUDY ON THE ROLE OF BRCA2 IN MITOSIS: SPINDLE ASSSEMBLY CHECKPOINT SIGNALING REGULATING BUBR1

III-8. BRCA2 complex in mitosis

Previous research with the acetylation deficient knock-in mouse model showed that acetylation of BubR1 is specifically required for maintaining MCC integrity and proper KT-MT attachment. But specifically which signaling factors influence BubR1 acetylation in mitosis needs to be analyzed in detail.

Considering the fact that only one kinetochore is enough to activate SAC and the turn-over rate of SAC proteins is fast, it is presumable that SAC signaling network is complex and meticulously designed. Many essential proteins such as kinases and phosphatases play important roles in initialization and extinguishment of SAC signaling. For example, Cdk1, Aurora B, Mps1 and Plk1 are representative kinases working at the forefront of SAC signaling. Phosphorylations by kinases on its target SAC proteins enable spatiotemporal regulation (Musacchio and Salmon, 2007). On the contrary, PP2A complex and PP1 mediated dephosphorylation promote mitotic exit (Wu.J.Q. et al., 2009; Grallert, A. et al., 2015).

It has been reported that BRCA2 is involved in acetylation of BubR1 at K250 by PCAF acetyltransferase in mitosis (Choi et al., 2012). But it is

unknown what licenses BRCA2 to kinetochores to full fill its function in mediating acetylation of BubR1. Also, whether BRCA2 acts beyond recruiting PCAF and BubR1 and fine tunes SAC signaling to maintain genomic integrity is another question.

To access how BRCA2 may be involved in mitotic signaling, targeted approach was taken to confirm and validate the BRCA2 complex specific to mitosis. Mitotic extracts were harvested after nocodazole treatment and immunoprecipitated with BRCA2. In mitosis, BRCA2 is phosphorylated, as reflected in the shift in gel electrophoresis. Cdk1 phosphorylates BRCA2 at S3291 and this specific phosphorylation inhibits interaction with RAD51 and interferes with recombination activity in mitosis (Esashi et al., 2005). Plk1 is another kinase which phosphorylates BRCA2 at the N-terminus (Lin et al., 2003) but how this phosphorylation of BRCA2 affects activity of BRCA2 in mitosis is unclear. BRCA2 co-precipitated with Plk1, BubR1 and PCAF acetyltransferase (Fig.17). As these proteins form a complex on phosphorylated BRCA2 specifically in mitosis, it may be possible that Plk1 phosphorylation of BRCA2 have a distinct effect on assembling the complex.

Figure 17

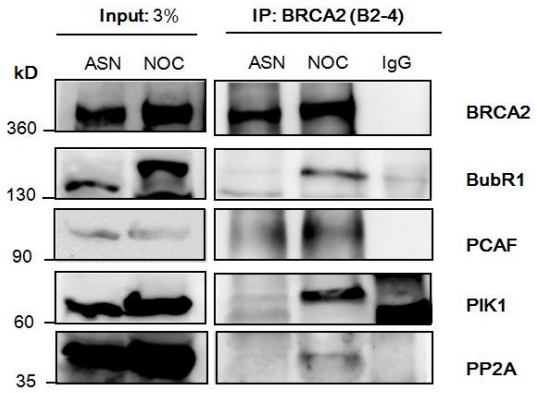

Fig.17 BRCA2 complex in mitosis

A comparison of BRCA2 interacting proteins in asynchronous cells and nocodazole treated mitotic cells. Cells were synchronized in mitosis by treating 200 ng/ml nocodazole after thymidine block and release. 3 mg of cell lysate was used for immunoprecipitation of BRCA2 with anti-B2-4 antibody coupled beads for 4 hr at 4℃.

In addition, SAC proteins required for the formation of APC/C-MCC did not co-immunoprecipitate with BRCA2 in mitosis. The APC/C subunit APC3, Bub3 and Mad2 were not detected (data not shown). This suggests that acetylated BubR1 leaves BRCA2 in order to form the MCC.

III-9. BRCA2 mediated BubR1 acetylation is required for the BubR1-HDAC interaction

BubR1 is deacetylated as cells exit mitosis (Choi et al., 2009). Previously, it was shown that under transient expression, BubR1 could interact with HDAC1, HDAC2 and HDAC3, which are all members of class I histone deacetylase family (Choi et al., 2009). Class I HDACs are ubiquitously expressed throughout the cell cycle and localize to the nucleus and cytoplasm (New et al., 2012). These HDACs have been suggested to play a role in mitosis, as HDAC inhibitors induce mitotic slippage (Stevens et al., 2008) and disrupt centromere function (Taddei et al., 2001). Interestingly, HDAC3 localizes to mitotic spindles and its enzymatic activity is important for chromosome alignment and the duration of mitosis. However, it does not deacetylate tubulin, nor histone H3K9, possibly suggesting the presence of another target (Ishii et al., 2008; Warrener et al., 2010). To verify HDAC3 interaction with endogenous BubR1 in mitosis, a cell line

expressing HDAC3-Flag-Venus at an endogenous level was generated. To verify HDAC2 interaction with BubR1, antibody specific to HDAC2 was used for immunoprecipitation. For comparison, asynchronous cells and mitotic cells enriched with taxol or nocodazole were used for immunoprecipitation. HDAC2 and HDAC3 interacted with BubR1, specifically in prometaphase when BubR1 is acetylated (Fig.18). As these HDACs specifically recognized acetylated BubR1, I tested the possibility of this interaction requiring BRCA2. When BRCA2 was depleted in mitotic cells, the interaction between the HDACs and BubR1 was disrupted (Fig.19).

.

Figure 18

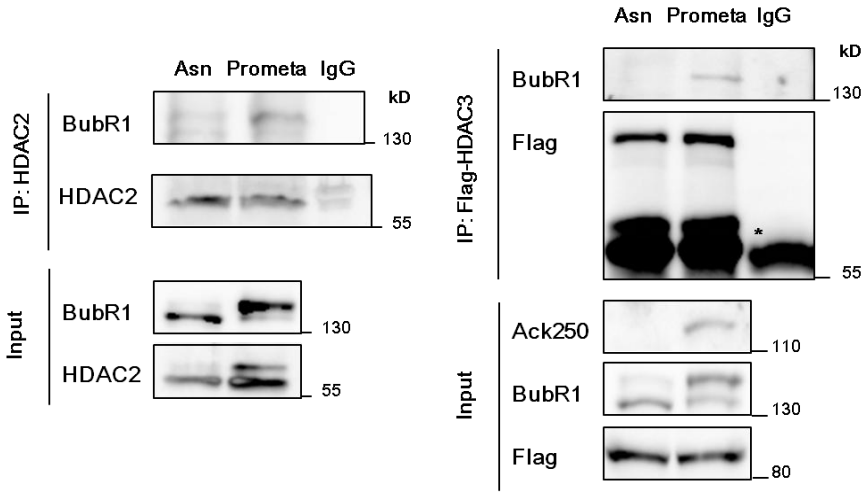
Asn Prometa IgG
kD
IP: HDAC2
BubR1
130
HDAC2
55
Input
BubR1
130
HDAC2
55
Asn Prometa IgG
kD
IP: Flag-HDAC3
BubR1
130
Flag
*
55
Input
Ack250
110
BubR1
130
Flag
80

Fig.18 HDAC2 and HDAC3 interact with BubR1 in prometaphase

Interaction between endogenous BubR1 and HDAC2/HDAC3 was assessed in asynchronous and prometaphase cells. 10 μM taxol or 200 ng/ml nocodazole was treated to arrest cells in prometaphase. 1 mg cell lysate was used for immunoprecipitation.

(Left) Endogenous HDAC2 was immunoprecipitated with the anti-HDAC2 antibody. 200 ng/ml nocodazole was treated to arrest cells in prometaphase. **(Right)** FRT/TO flip-in HeLa cells expressing HDAC3-flag-venus was treated with 1 μg/ml doxycycline to induce HDAC3 expression. Endogenous HDAC3 was depleted with siRNA targeting 3′UTR. 10 μM taxol was treated to arrest cells in prometaphase. HDAC3 was immunoprecipitated using the flag coupled beads.

* non specific band

Figure 19

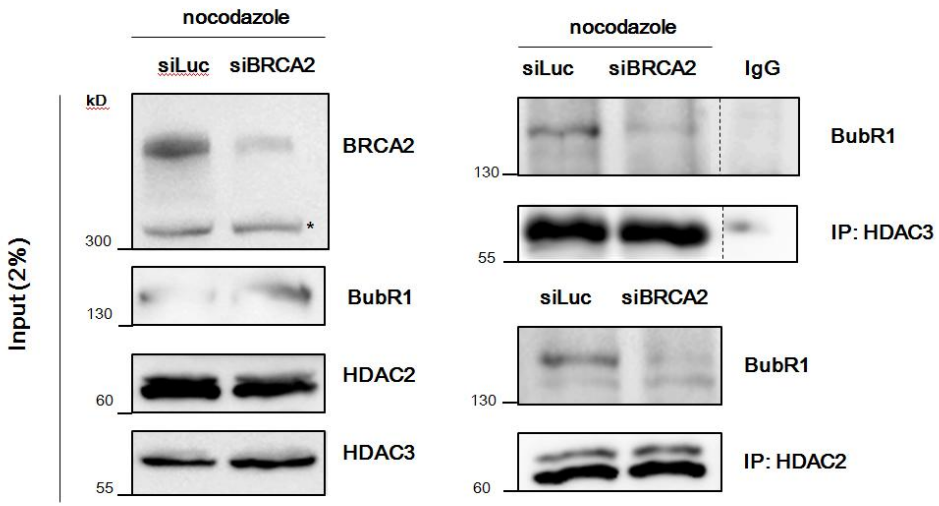

Figure.19 HDAC2 and HDAC3 interact with BubR1 in the presence of BRCA2 at prometaphase

siBRCA2 or siluciferase was transfected to HeLa cells. Cells were arrested in prometaphase by treating 200 ng/ml nocodazole for 12 hr. Mitotic cells were harvested by mechanical shake off. 2 mg of cell lysate was immunoprecipitated with anti-HDAC2 or anti-HDAC3 antibody.

III-10. BubR1 deacetylation is a cue to SAC silencing

To access if deacetylation of BubR1 could act as a signal for SAC silencing, the fate of cells expressing BubR1 acetylation deficient (K250R) and mimicking mutant (K250Q) was analyzed by time lapse microscopy. Studies with cells lacking P31 comet or APC15, which are specific regulators in silencing the SAC, have pointed out that in addition to lengthened mitotic timing; prolonged metaphase is a phenotype indicative of mitotic exit problem (Westhorpe et al., 2011; Mansfeld et al., 2011).

Endogenous BubR1 was silenced by targeting 3′UTR with siRNA and mcherry tagged BubR1 K250R or K250Q mutants were co-expressed. In mitosis, acetylation deficient BubR1 is susceptible to ubiquitination and is prematurely degraded (Choi et al., 2009). As expected, expression of K250Q mutant resided in mitosis for a longer period. But strikingly, metaphase was lengthened in these cells; even though mature bipolar KT-MT attachment was accomplished (Fig.20).

To access if this metaphase delay was a result of BubR1 acetylation functioning through SAC and not due to defective APC/C activity, kinetochore dependent pathway was blocked with Mps1 inhibitor reversine (Santaguida et al., 2010). Treatment with 0.5 μM reversine eliminated the metaphase delay in K250Q expressing cells (Fig.21) which indicates that in the absence of SAC, APC/C activity is likely equal in siLuc treated control

cells and BubR1 depleted cells rescued with K250Q. As acetylation status affects the integrity of MCC (Fig.9), it could be inferred that MCC disassembly is affected. This result suggests that deacetylation of BubR1 is a cue to SAC silencing.

Figure 20

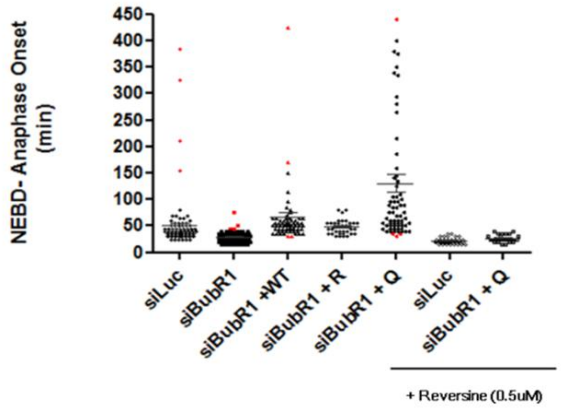

Fig.20 Analysis on the APC/C activity in cells expressing BubR1 K250Q

H2B-GFP HeLa cells were transfected with siBubR1 3′UTR and pcDNA3.1-mcherry BubR1 plasmids. After 6 hr of release from thymidine block, cells were filmed with time lapse microscopy in 5 min intervals, for total of 24 hr. On average, single cell intensity of mcherry-BubR1 was comparable among the mutants. n>50 cells were analyzed per mutants. Outliers are shown in red.

Figure 21

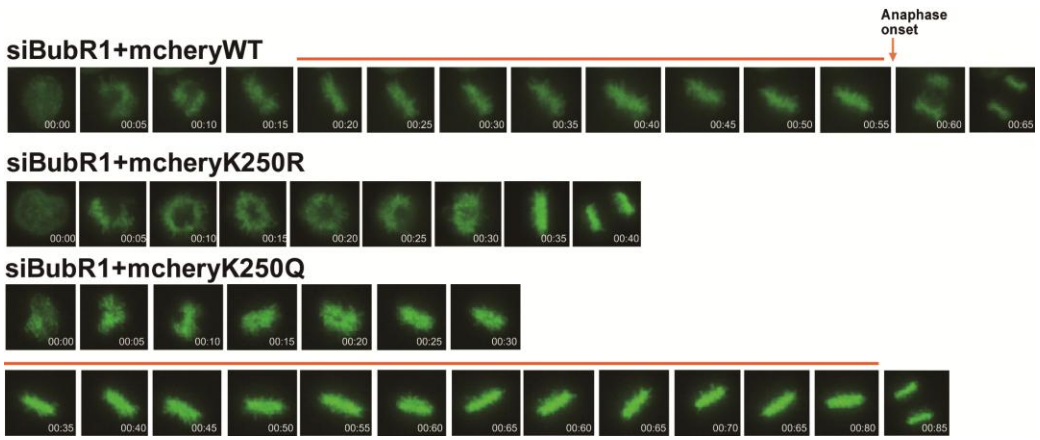
Anaphase onset
siBubR1+mcheryWT
00:00 00:05 00:10 00:15 00:20 00:25 00:30 00:35 00:40 00:45 00:50 00:55 00:60 00:65
siBubR1+mcheryK250R
00:00 00:05 00:10 00:15 00:20 00:25 00:30 00:35 00:40
siBubR1+mcheryK250Q
00:00 00:05 00:10 00:15 00:20 00:25 00:30
00:35 00:40 00:45 00:50 00:55 00:60 00:65 00:60 00:65 00:70 00:65 00:80 00:85

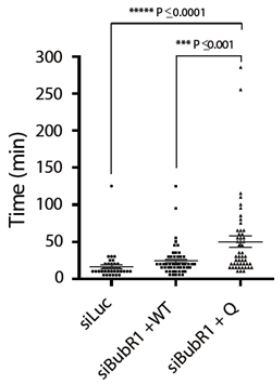
***** P ≤0.0001
*** P ≤0.001
Time (min)
300
250
200
150
100
50
0
siLuc
siBubR1 +WT
siBubR1 + Q

Fig.21 Metaphase delay occurs when acetylation is prolonged in cells

Captured images of representative cells expressing the BubR1 mutants (K250, K250R and K250Q) from NEBD to anaphase onset. Each frame is in 5 min interval. Metaphase is depicted in an orange line. The graph on the right represents the duration of metaphase before anaphase onset.

To validate if BubR1 deacetylation is under the control of canonical SAC signaling, acetylation of BubR1 was monitored in the conditions mimicking SAC silencing. Previous studies showed that when cells are blocked in mitosis with MG132 only, despite the fact that chromosomes are aligned at the metaphase plate, MCC still exists and APC/C remains inactive, indicating that SAC is not silenced in this condition (Jia et al., 2011). Reversine is an inhibitor of Mps1 kinase and hesperadin is an inhibitor of Aurora B kinase. The combinatorial use of either reversine or hesperadin with MG132 faithfully mimics the SAC silenced state as MCC readily disassemble and APC/C-Cdc20 is activated (Jia et al., 2011; Mansfeld et al., 2011). To chemically recapitulate SAC silencing at kinetochores, cells were arrested in prometaphase with taxol and sequentially released into media containing different combination of drugs. MG132 (blocks degradation of Securin and Cyclin B) was used to maintain cells in mitosis and reversine or hesparadin was used to shut down the kinetochore signaling (Jia et al., 2011; Santaguida et al., 2011; Mansfeld et al., 2011). Acetylation of BubR1 decreased in mitotic extracts (+MG132) deprived of Mps1 or Aurora B activity, in concert with dephosphorylation of BubR1 (Fig.22). Hence, BubR1 is deacetylated when SAC signaling is turned off at kinetochores in mitosis and acetylation is regulated in parallel with phosphorylation of BubR1.

Figure 22

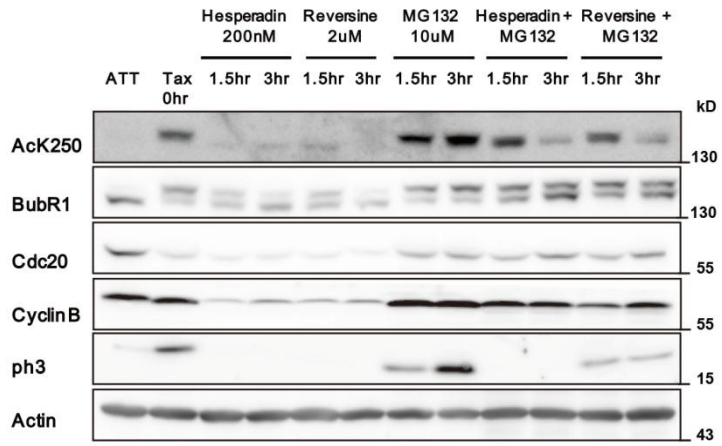

Fig.22 BubR1 is deacetylated upon SAC silencing in mitosis

HeLa cells were synchronized with a single thymidine block and released into G_2/M phase of the cell cycle. After 7 hr of release, cells were treated with 10 μM taxol. Mitotic cells were enriched with mechanical shake off and were further released into media containing the combination of drugs. 10 μM MG132, 2 μM reversine, 200 nM hesperadin was used. Cells were harvested after 1.5 or 3 hr.

Previous blot showed that acetylation-phosphorylation and deacetylation-dephosphorylation of BubR1 work in parallel during mitosis. Studies have suggested that in mitosis BubR1 is phosphorylated by Plk1 (Elowe et al., 2007; Matsumura et al., 2007) and Aurora B (Ditchfield et al., 2003; Hauf et al., 2003). Among the many phosphorylated residues, phosphorylation of BubR1 at 670, 676 serine and 680 threonine are suggested to be involved in chromosome alignment (Elowe et al., 2007; Huang et al., 2008; Suijkerbuijk et al., 2012). These residues are grouped nearby, forming the KARD domain and regulate KT-MT attachment through recruiting PP2AB56a to counterbalance Aurora B activity (Suijkerbuijk et al., 2012). As acetylation of BubR1 was specifically involved in KT-MT attachment through PP2AB56a recruitment along with SAC activity, the idea of possible sequential regulation of K250 acetylation and KARD domain phosphorylation was tested. Constructs with both acetylation and phosphorylation mutations were made. K250 was mutated to either acetylation deficient argentine (R) or acetylation mimicking glutamine (Q). The S670, S676, T680 sites in the KARD domain were all mutated to phosphorylation deficient aspartic acid (A) or phosphorylation mimicking alanine mutant (D).

First, H2B-GFP HeLa cells were depleted of endogenous BubR1 and rescued with double mutants of acetylation and phosphorylation. BubR1 acetylation mutants (WT, K250R and K250Q) had the KARD phosphorylation sites mutated to phosphorylation deficient (3A) or phosphorylation mimicking form (3D). Timelapse microscopy analysis was done to analyze both mitotic timing and chromosome congression. The hypothesis was that as KARD domain phosphorylation mainly contributes to chromosome alignment (Suijkerbuijk et al., 2012), mitotic timing would be determined by the acetylation status. When key residues of KARD domain were all mutated to phosphorylation deficient form (3A), most cells were blocked in mitosis with severe chromosome alignment defects (Fig.23a,c). This was indifferent when acetylation was deficient or enforced at the same time (Fig.23b).

Unexpectedly, as seen from cells expressing phosphorylation mimicking mutant W3D, KARD phosphorylation itself seemed to activate SAC as mitotic timing was extended compared to control cells rescued with WT BubR1 (Fig.23a). Percentage of cells with normal congression was comparable to that of WT. This suggests that phosphorylation itself actually affects SAC signaling and this may be possible as S760 is also regulated by Mps1 kinase (Huang et al., 2008). It was hard to tell apart the effect of acetylation in either mitotic timing or congression, making it difficult to

determine the sequence of events (Fig.23b). SAC regulation was juxtaposed when all three residues in KARD domain was simultaneously mutated, possibly suggesting an order of regulation within these residues.

Figure 23

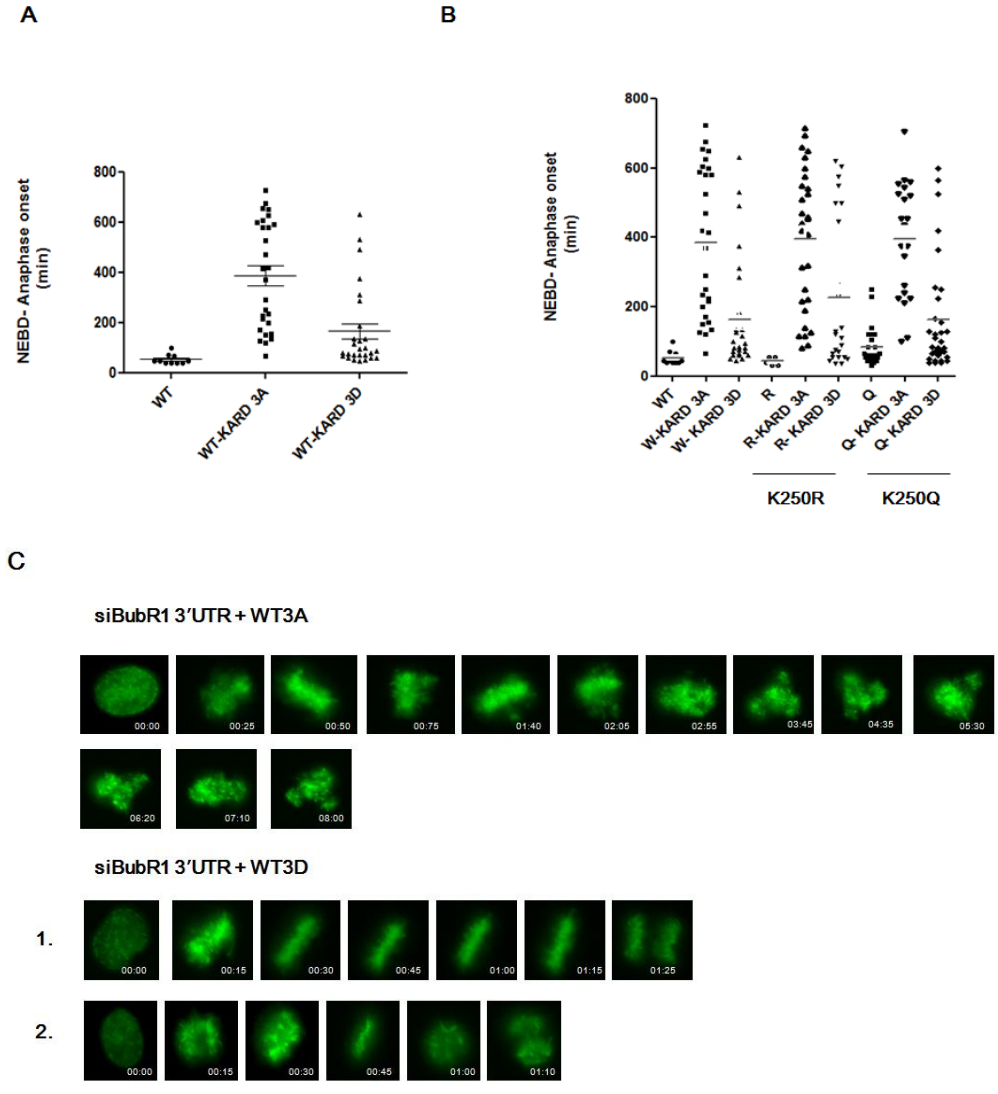
A
NEBD- Anaphase onset (min)
800
600
400
200
0
WT
WT-KARD 3A
WT-KARD 3D
B
NEBD- Anaphase onset (min)
800
600
400
200
0
WT
W-KARD 3A
W- KARD 3D
R
R-KARD 3A
R- KARD 3D
Q
Q- KARD 3A
Q- KARD 3D
K250R
K250Q
C
siBubR1 3′UTR + WT3A
00:00
00:25
00:50
00:75
01:40
02:05
02:55
03:45
04:35
05:30
06:20
07:10
08:00
siBubR1 3′UTR + WT3D
1.
00:00
00:15
00:30
00:45
01:00
01:15
01:25
2.
00:00
00:15
00:30
00:45
01:00
01:10

Fig.23 Mitotic timing of cells expressing BubR1 acetyl-KARD 3A/3D mutants

H2B-GFP HeLa cells were depleted of endogenous BubR1 by siRNA targeting 3′UTR of BubR1. pcDNA3.1-mcherry BubR1 mutants were co-transfected. Cells were synchronized in S phase by thymidine block and released into G2/M phase at the time of filming. **(A)** Mitotic timing of cells expressing phosphorylation mimicking (3D) or phosphorylation deficient (3A) mutants. **(B)** Mitotic timing of cells expressing mutants of both BubR1 acetylation and KARD phosphorylation. **(C)** Captured images of two different representative cells expressing WT- KARD3A or WT- KARD3D.

To simplify the matter, single phosphorylation site was targeted in concert with the acetylation site. T680 is directly phosphorylated by Plk1 (Suijkerbuijk et al., 2012) and is essential for KT-MT attachment. Single phosphorylation deficient mutation at T680 (WT-KARD680A) lengthened mitotic timing consistent with presence of unaligned chromosomes. However, eventhough cells expressing the WT-KARD680D mutant congressed properly, mitotic timing was shortened, which may imply SAC was silenced faster (Fig.24a). This too suggests another pathway other than Plk1 mediated signaling could be involved when T680 phosphorylation is constantly enforced or absent. Hence, single site targeting of phosphorylation could also affect SAC activity in away, apart from KT-MT attachment. In conclusion, live analysis data reflected that SAC signaling network is complex and although acetylation and phosphorylation of BubR1 act in concert, the sequential activation and silencing between the two signals cannot be specified.

Figure 24

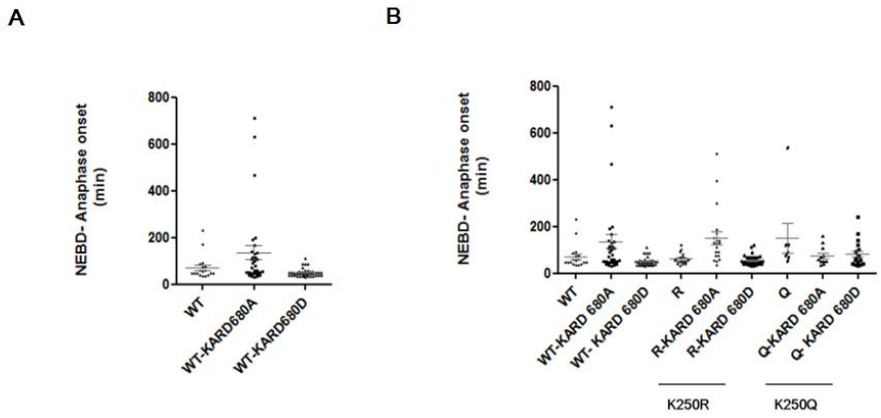

Fig.24 Mitotic timing of cells expressing BubR1 acetylation-phosphorylation mutants

H2B-GFP HeLa cells were depleted of endogenous BubR1 by siRNA targeting 3´UTR of BubR1. **(A)** Mitotic timing of cells rescued with BubR1 680T phosphorylation mutants. **(B)** Mitotic timing of cells expressing double mutants of K250 acetylation and 680T phosphorylation.

NEBD is set to 00:00 min.

IV. Discussion

IV-1. Dual roles of BubR1 acetylation and tumorigenesis

In eukaryotes, BubR1 is a central component of SAC, which is a surveillance mechanism ensuring bipolar segregation of chromosomes in anaphase (Mussachio and Salmon, 2007). In prometaphase, BubR1 is acetylated at K250 by PCAF through BRCA2 interaction (Choi et al., 2009; Choi et al., 2012). These previous studies have suggested that acetylation of BubR1 is integral to protecting the protein from ubiquitination and SAC activity. Also, possible tumor-suppressive role of BubR1 acetylation was inferred from the tumorigenesis occurring in B2-9 transgenic mouse model (Choi et al., 2012). But how acetylation of BubR1 acts within SAC and its *in vivo* significance is unknown. Through the study with BubR1 acetylation deficient knock-in mouse model (*K243R/+*), I suggest that BubR1 acetylation is specifically involved in 1) the maintenance of the MCC formed and 2) KT-MT attachment (Fig.25).

Figure 25

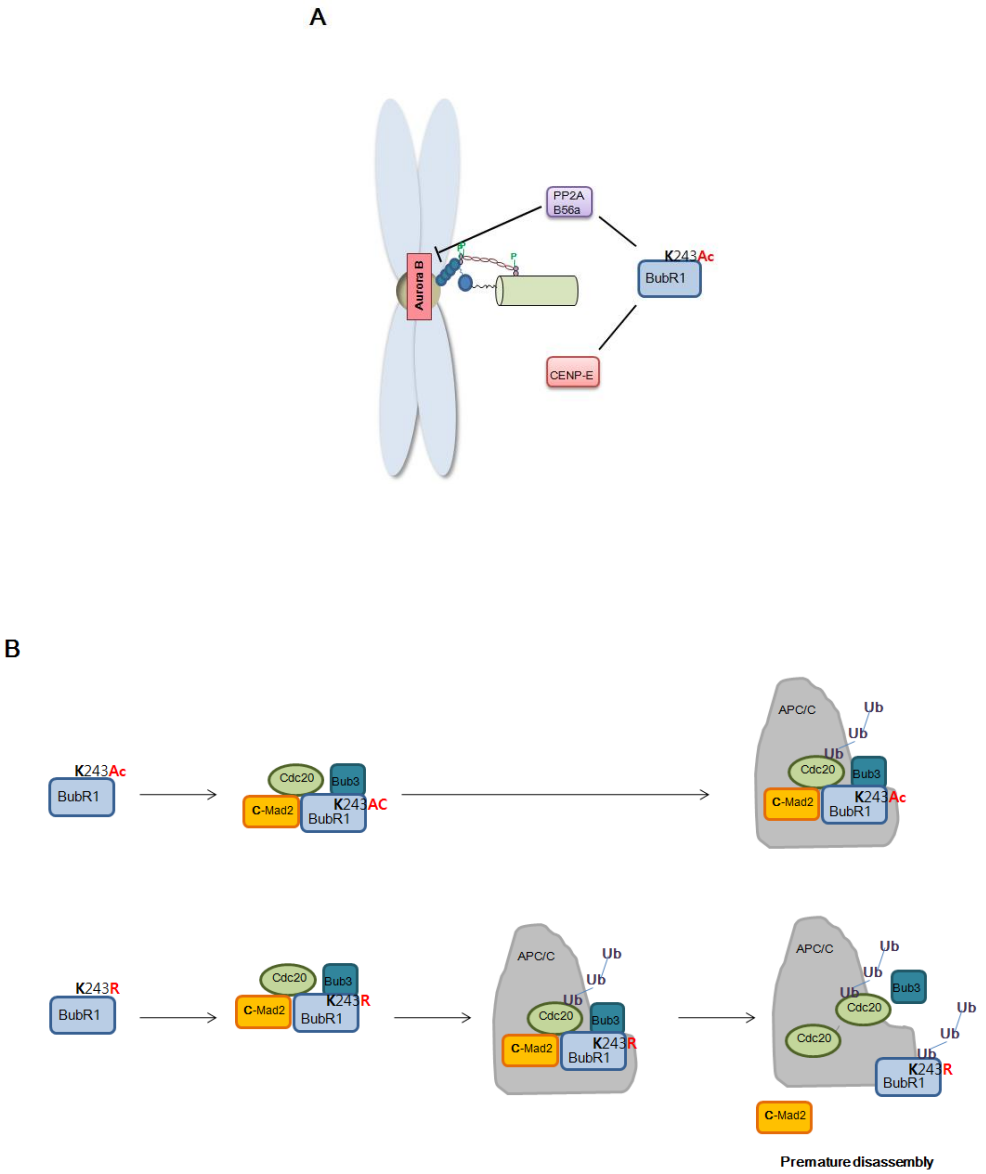
A
PP2A
B56a
Aurora B
K243Ac
BubR1
CENP-E
B
K243Ac
BubR1
Cdc20
Bub3
C-Mad2
K243AC
BubR1
APC/C
Ub
Ub
Ub
Cdc20
Bub3
C-Mad2
K243Ac
BubR1
K243R
BubR1
Cdc20
Bub3
C-Mad2
K243R
BubR1
APC/C
Ub
Ub
Ub
Cdc20
Bub3
C-Mad2
K243R
BubR1
APC/C
Ub
Ub
Ub
Bub3
Cdc20
Ub
Cdc20
Ub
K243R
BubR1
C-Mad2
Premature disassembly

Fig.25 BubR1 acetylation is required for stable KT-MT attachment and MCC maintenance.

(A) *K243R/+* cells exhibit congression failure because 50% of BubR1 is acetylation deficient. Acetylation-deficient BubR1 (K243R) is incapable of recruiting PP2AB56a to counterbalance Aurora B kinase activity at the KMN network, and this process is crucial for stable KT–MT interaction. K243R also has reduced CENP-E binding (data not shown), which may contribute to the problem in chromosome congression.

(B) Half of the SAC complex contains K243R-BubR1 and fails to maintain SAC activity. K243R associates with other MCC components; however, the protein is readily ubiquitinated by the APC/C, resulting in disassociation of MCC. As initial SAC signal generation is intact, premature disassembly of MCC leads to failure in the maintenance of SAC, effectively weakening SAC activity. The combined effects of chromosome–spindle attachment failure and weakened SAC lead to massive chromosome mis-segregation and initiate tumorigenesis in *K243R/+* mice.

IV-1-1. BubR1 acetylation deficiency results in premature disassembly of MCC

In *K243R/+* cells, the level of Mad1 and Mad2 recruited to kinetochores were comparable to that of WT at prometaphase, which indicates that signals priming the MCC formation are intact (Fig.7). But MCC formed in *K243R/+* prometaphase cells disassembled even though SAC was activated by nocodazole. Under this nocodazole treated condition, a similar amount of BubR1 was immunoprecipitated as in WT cells to compare MCC bound to BubR1. The disassembly of Mad2, Bub3 and Cdc20 was further rescued with MG132 treatment, implying that K243R-BubR1 affects how MCC is held together (Fig.9). In essence, upon SAC activation, recruited MAD proteins at kinetochore catalyze the formation of MCC but after formation, presence of deacetylated BubR1 within the complex disrupts the maintenance of MCC throughout mitosis.

Considering the fact that *K243R/+* MEFs expressed WT-BubR1 and K243R-BubR1 protein at 1:1 ratio in mitosis (Fig.9a) and higher level of BubR1 is recruited to kinetochores compared to *BubR1*$^{+/-}$ MEFs, the acetylation-deficient *BubR1* allele functions as a dominant allele in SAC maintenance and KT-MT attachment. It is clear that acetylation of BubR1 is necessary for maintaining the MCC, and further question of whether deacetylation is indeed a direct cue to SAC silencing is addressed in this

study. Once SAC proteins are ubiquitinated by APC/C E3 ligase (Musacchio and Salmon, 2007), they leave APC/C to be degraded by 26S proteasome in the cytosol. I imagine, as deacetylation of BubR1 occurs prior to ubiquitination of the protein (Choi et al., 2009) and deacetylation of BubR1 affects disassembly of MCC proteins from APC/C, deacetylation triggers structural change in BubR1 which disrupts molecular interactions within the MCC. In line of this, it would be interesting to model the structural difference between the acetylated and deacetylated form of BubR1.

IV-I-2. BubR1 acetylation deficiency disrupts stable kinetochore-microtubule attachment

K243R-BubR1 localizes to kinetochores (Fig.8) and chromosome alignment defects occur at high incidence in *K243R/+* MEFs (Fig.10). To guarantee stable KT-MT attachment and error correction, Aurora B activity of phosphorylating the KMN network needs to be regulated at a balanced level. BubR1 has been suggested to bind to PP2AB56a subunit of PP2A phosphatase after phosphorylation at KARD domain (Suijkerbuijk et al., 2012; T.Kruse et al., 2013). From this study, I have elucidated that KT-MT attachment defects in *K243R/+* arise from imbalance in Aurora B activity, due to reduced recruitment of PP2AB56a (Fig.13). This suggests the possible cross talk between phosphorylation of KARD domain and

acetylation of BubR1 at 243th lysine.

Collectively, when *K243R/+* cells proceeded through mitosis, the probability of making erroneous KT-MT attachments were high, but shortened duration of SAC prompted chromosomes to segregate despite the presence of unstable KT-MT attachments. Hence, lagging chromosomes occurred at high incidence of 15% in *K243R/+* MEFs, which could be a direct source for micronuclei that also appeared 3 fold higher than WT (data not shown). It has been suggested that errors in mitosis and the resulting micronuclei could be a source of chromothripsis, the shattering of chromosomes. Also, as micronuclei undergo asynchronous and defective DNA replication (Crasta et al., 2012), they could stimulate local genetic alterations to occur. Indeed, after multiple rounds of cell division, CIN manifested in forms of aberrant number and structure of chromosomes, which may accompany genetic alterations favoring tumorigenesis. In effect, p53 mutations frequently occurring in human tumors were detected in *K243R/+* tumors (data not shown).

The answer to the question of whether aneuploidy is a result or cause of tumorigenesis is addressed through this study on *K243R/+* mice. *BubR1*$^{+/-}$ resulted in abnormal megakaryopoiesis, but spontaneous cancer development was not observed (Wang et al., 2004). Unexpectedly, BubR1 insufficiency in *BubR1*$^{H/H}$ succumbed to premature aging phenotype (Baker

et al., 2004). In comparison, *K243R/+* mice did not show any premature aging phenotype but a high incidence of spontaneous tumorigenesis occurred in solid and hematologic tissues (Table.2). These differences show that effects by deacetylation of BubR1 are not simply due to decrease in protein level in mitosis. Specifically, in chromosome congression analysis, *K243R/+* MEFs displayed significant defects in KT-MT attachments than *BubR1*$^{+/-}$ MEFs. As *BubR1*$^{+/-}$ and *BubR1*$^{H/H}$ MEFs also harbor aneuploidy, whole chromosome aneuploidy alone cannot be the cause for spontaneous tumorigenesis.

Mutations of SAC regulators have been reported in human cancer by genetic or epigenetic means (I.Perez de Castro et al., 2007). It is interesting to note that single arginine mutation at 250th lysine of human BubR1 can be tumorigenic, as conserved 243th lysine mutated to arginine in mice lead to cancer predisposition. Further analysis of whether acetylation mutation of BubR1 occurs in human tumors and if other mutations of BubR1 affect the 250th lysine acetylation should be carried out.

IV-2. BubR1 acetylation/deacetylation in SAC signaling network

Through this study, I have shown that BubR1 deacetylation is an active signal to SAC silencing (Fig.21 and Fig.22). As evident from studies with cells lacking P31 comet or APC15, which are specific regulators in silencing the mitotic checkpoint through regulation of MCC disassembly, prolonged metaphase is a typical phenotype indicative of mitotic exit problem (Westhorpe et al., 2011; Mansfeld et al., 2011). When endogenous BubR1 was depleted and acetylation mimicking mutant was expressed in cells, metaphase was delayed in addition to extended mitotic timing (Fig.21). This point out that deacetylation is a cue for SAC silencing and could also be a direct cue to disassembly of MCC. The steps into how MCC disassembly occurs is unclear, but it would be interesting to test if deacetylation of BubR1 acts in concord with P31 comet or APC15.

In addition, when SAC is silenced in mitosis by targeting Mps1 and Aurora B kinase required for SAC activation, BubR1 was deacetylated (Fig.22). This suggests that deacetylation of BubR1 acts within the canonical SAC signaling pathway. But it still remains to be known when and where BubR1 is acetylated and deacetylated in the cell. I believe better insight into spatiotemporal regulation of BubR1 acetylation could be done with antibody that works for IFA (in the progress of screening) and through analysis of

primary cell genetically engineered to have the BubR1 K250R-GFP allele.

As K250 acetylation and KARD domain phosphorylation of BubR1 both affects chromosome alignment, the possibility of these modifications acting in a sequence was tested. However, the approach with live imaging analysis showed that phosphorylation in the KARD domain itself also affects SAC activity (Fig.23 and Fig.24), which might be attributed by various roles of Plk1 phosphorylation in SAC signaling. Furthermore, existence of various cues other than post-translational modification of BubR1 makes it hard to isolate and examine the sequential activation between the signals during SAC.

IV-3. BRCA2 is a hub for SAC silencing: a hub for BubR1 modulation

A method in which cells achieve specificity in their molecular signaling networks is to organize discrete subsets of proteins in space and time. This can be achieved through utilizing proteins acting as “scaffold”. BRCA2 is a multi domain protein, which interacts with PCAF at the C-terminus and BubR1 at the N-terminus in prometaphase (Choi et al., 2012). Analysis on the proteins interacting with BRCA2 in mitosis suggested the possibility that BRCA2 is not only required for recruitment of BubR1 and PCAF together for acetylation of BubR1 (Fig.17). An interesting fact is that Plk1 co-immunoprecipitated with BRCA2-BubR1. How BRCA2 localizes to kinetochores and what activates the assembly of PCAF and BubR1 on BRCA2 is unknown, but Plk1 may be a good candidate considering the fact that it phosphorylates BRCA2 before entry into mitosis at N-terminus and within the BRC repeat region (Lin et al., 2003; Lee et al., 2004; Takaoka et al., 2014).

Specific to prometaphase, HDAC2 and HDAC3 interacted with endogenous BubR1 (Fig.18 and Fig.19). HDAC2 and HDAC3 have broad range of localization in prometaphase, diffuse throughout the cytoplasm (He et al., 2012). The interaction between HDACs and BubR1 was intact only if BRCA2 was present in prometaphase cell extracts (Fig.19), which suggests

that BRCA2 helps class I HDACs to be specifically recruited to BubR1 at kinetochores in prometaphase. As class I HDACs (HDAC1, HDAC2 and HDAC3) share the conserved deacetylase domain and localize in cytoplasm, they seem to share a redundant role in deacetylating BubR1 in mitosis. Detection of PP2AC may also suggest possible interaction between BRCA2 and functional regulatory B subunits of PP2A, implicated in dephosphorylation activities in mitosis (Fig.17). If PP2AB56a co-immunoprecipitates with BRCA2 mitotic complex, it would imply that BRCA2 extends beyond mediating acetylation and deacetylation of BubR1 to regulate BubR1 signaling in SAC. More profound analysis on the mitotic complex could be carried out through mass spectrometry analysis to compare the difference in interacting proteins by using the acetylated and deacetylated BubR1 as baits.

As BRCA2 only localizes to kinetochores in prometaphase, it is likely that Plk1, BubR1 and class I HDACs all co-localize to kinetochores. Such confined localization of the proteins could enhance the efficiency of acetylation and deacetylation switch of BubR1 and ultimately, SAC signaling in prometaphase. Furthermore, the regulatory role of BRCA2 as a scaffold in mitosis and tumor suppressive characteristics of BubR1 acetylation suggest BubR1 acetylation as an attractive target for BRCA2 mutated cancers.

Cancer cells in general show deregulation in cell-cycle and anti-mitotic therapies have been suggested effective against the abnormal proliferation of transformed cells (Chan et al., 2012). Taxane (or taxol) is one of the anti-mitotic drugs proven to be successful in clinics. But taxane could also target quiescent cancer cells because of the importance of microtubule dynamics in cells not undergoing mitosis (Mitchison, 2012). Hence, more selective strategies targeting mitosis are in a need. I suggest that as Plk1 and HDACs cooperate with BRCA2 in mitosis, possibly Plk1 inhibitor BI2536 (Boehringer Ingelheim Inc.) and HDAC inhibitors in combination could selectively killing cancer cells with BubR1 or BRCA2 mutation. This should be tested with cancer cells with BRCA2 mutations.

Figure 26

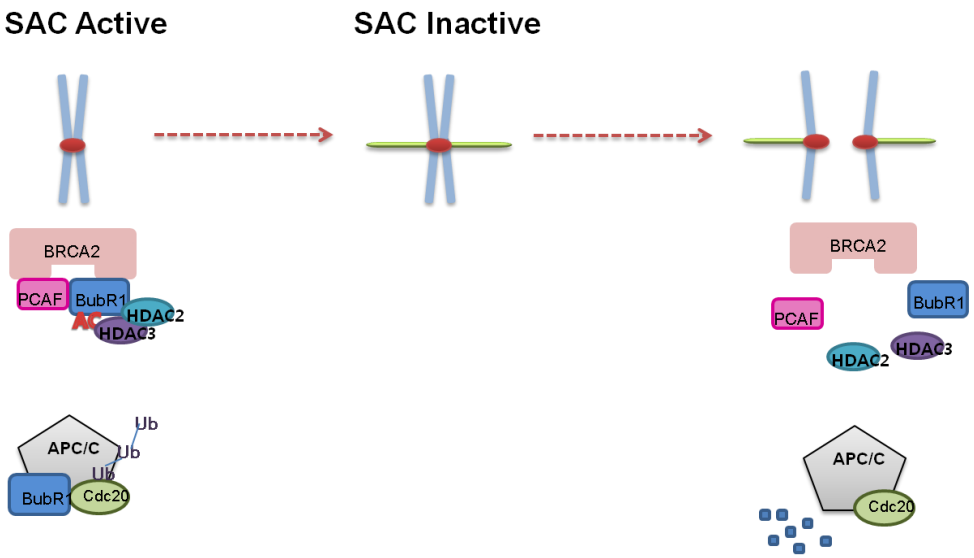
SAC Active
SAC Inactive
BRCA2
PCAF
BubR1
HDAC2
HDAC3
Ac
Ub
Ub
Ub
APC/C
BubR1
Cdc20
BRCA2
PCAF
BubR1
HDAC2
HDAC3
APC/C
Cdc20

Fig. 26 BRCA2 is the scaffold for BubR1 acetylation/deacetylation

In prometaphase, when SAC is active, BRCA2 localizes to kinetochores with BubR1 and PCAF. Direct interaction of BRCA2 with BubR1 and PCAF at the N-terminus and C-terminus respectively, mediate acetylation of K250 BubR1. The acetylated BubR1 presented by BRCA2, recruits HDAC2/3 to BubR1. Followed by HDAC2/3-BubR1 interaction, BubR1 is deacetylated as SAC is silenced.

V. Reference

Basu, J., H. Bousbaa, E. Logarinho, Z. Li, B. C. Williams, C. Lopes, C. E. Sunkel and M. L. Goldberg (1999). "Mutations in the essential spindle checkpoint gene bub1 cause chromosome missegregation and fail to block apoptosis in Drosophila." J Cell Biol 146(1): 13-28.

Buffin, E., C. Lefebvre, J. Huang, M. E. Gagou and R. E. Karess (2005). "Recruitment of Mad2 to the kinetochore requires the Rod/Zw10 complex." Curr Biol 15(9): 856-861.

Chan K-S, Koh C-G, Li H-Y (2012). "Mitosis-targated anti-cancer therapies: where they stand." Cell Death and Disease (2012) 3, e411; doi:10.1038/cddis.2012.148

Chao, W. C., K. Kulkarni, Z. Zhang, E. H. Kong and D. Barford (2012). "Structure of the mitotic checkpoint complex." Nature 484(7393): 208-213.

Choi, E., H. Choe, J. Min, J. Y. Choi, J. Kim and H. Lee (2009). "BubR1 acetylation at prometaphase is required for modulating APC/C activity and timing of mitosis." EMBO J 28(14): 2077-2089.

Choi, E., P. G. Park, H. O. Lee, Y. K. Lee, G. H. Kang, J. W. Lee, W. Han, H. C. Lee, D. Y. Noh, S. Lekomtsev and H. Lee (2012). "BRCA2 fine-tunes the spindle assembly checkpoint through reinforcement of BubR1 acetylation." Dev Cell 22(2): 295-308.

Crasta K., Ganem N.J., Dagher R., Lantermann A.B., Ivanova E.V., Pan Y., Nezi L., Protopopov A., Chowdhury D., and Pellman D. (2012) "DNA breaks and chromosome pulverization from errors in mitosis."Nature 482, 53-58.

Crook, T., L. A. Brooks, S. Crossland, P. Osin, K. T. Barker, J. Waller, E. Philp, P. D. Smith, I. Yulug, J. Peto, G. Parker, M. J. Allday, M. R. Crompton and B. A. Gusterson (1998). "p53 mutation with frequent novel condons but not a mutator phenotype in BRCA1- and BRCA2-associated breast tumours." Oncogene 17(13): 1681-1689.

D'Arcy, S., O. R. Davies, T. L. Blundell and V. M. Bolanos-Garcia (2010). "Defining the molecular basis of BubR1 kinetochore interactions and APC/C-CDC20 inhibition." J Biol Chem 285(19): 14764-14776.

DeLuca, K. F., S. M. Lens and J. G. DeLuca (2011). "Temporal changes in Hec1 phosphorylation control kinetochore-microtubule attachment stability during mitosis." J Cell Sci 124(Pt 4): 622-634.

Di Fiore, B., N. E. Davey, A. Hagting, D. Izawa, J. Mansfeld, T. J. Gibson and J. Pines (2015). "The ABBA motif binds APC/C activators and is shared by APC/C substrates and regulators." Dev Cell 32(3): 358-372.

Diaz-Martinez, L. A., W. Tian, B. Li, R. Warrington, L. Jia, C. A. Brautigam, X. Luo and H. Yu (2015). "The Cdc20-binding Phe box of the spindle checkpoint protein BubR1 maintains the mitotic checkpoint complex during mitosis." J Biol Chem 290(4): 2431-2443.

Ditchfield, C., V. L. Johnson, A. Tighe, R. Ellston, C. Haworth, T. Johnson, A. Mortlock, N. Keen and S. S. Taylor (2003). "Aurora B couples chromosome alignment with anaphase by targeting BubR1, Mad2, and Cenp-E to kinetochores." J Cell Biol 161(2): 267-280.

Elowe, S., S. Hummer, A. Uldschmid, X. Li and E. A. Nigg (2007). "Tension-sensitive Plk1 phosphorylation on BubR1 regulates the stability of kinetochore microtubule interactions." Genes Dev 21(17): 2205-2219.

Esashi, F., N. Christ, J. Gannon, Y. Liu, T. Hunt, M. Jasin and S. C. West (2005). "CDK-dependent phosphorylation of BRCA2 as a regulatory mechanism for recombinational repair." Nature 434(7033): 598-604.

Foley, E. A. and T. M. Kapoor (2013). "Microtubule attachment and spindle assembly checkpoint signalling at the kinetochore." Nat Rev Mol Cell Biol 14(1): 25-37.

Grallert, A., E. Boke, A. Hagting, B. Hodgson, Y. Connolly, J. R. Griffiths, D. L. Smith, J. Pines and I. M. Hagan (2015). "A PP1-PP2A phosphatase relay controls mitotic progression." Nature 517(7532): 94-98.

Hardwick, K. G., R. C. Johnston, D. L. Smith and A. W. Murray (2000). "MAD3 encodes a novel component of the spindle checkpoint which interacts with Bub3p, Cdc20p, and Mad2p." J Cell Biol 148(5): 871-882.

Hauf, S., R. W. Cole, S. LaTerra, C. Zimmer, G. Schnapp, R. Walter, A. Heckel, J. van Meel, C. L. Rieder and J. M. Peters (2003). "The small molecule Hesperadin reveals a role for Aurora B in correcting kinetochore-

microtubule attachment and in maintaining the spindle assembly checkpoint." J Cell Biol 161(2): 281-294.

Hoque, M. T. and F. Ishikawa (2002). "Cohesin defects lead to premature sister chromatid separation, kinetochore dysfunction, and spindle-assembly checkpoint activation." J Biol Chem 277(44): 42306-42314.

Howell, B. J., B. F. McEwen, J. C. Canman, D. B. Hoffman, E. M. Farrar, C. L. Rieder and E. D. Salmon (2001). "Cytoplasmic dynein/dynactin drives kinetochore protein transport to the spindle poles and has a role in mitotic spindle checkpoint inactivation." J Cell Biol 155(7): 1159-1172.

Huang, H., J. Hittle, F. Zappacosta, R. S. Annan, A. Hershko and T. J. Yen (2008). "Phosphorylation sites in BubR1 that regulate kinetochore attachment, tension, and mitotic exit." J Cell Biol 183(4): 667-680.

Ignacio Pe´rez de Castro, Guillermo de Ca´rcer and Marcos Malumbres (2007). "A census of mitotic cancer genes: new insights into tumor cell biology and cancer therapy." Carcinogenesis 28 (5): 899–912

Ishii, S., Y. Kurasawa, J. Wong and L. Y. Yu-Lee (2008). "Histone deacetylase 3 localizes to the mitotic spindle and is required for kinetochore-microtubule attachment." Proc Natl Acad Sci U S A 105(11): 4179-4184.

Kapanidou, M., S. Lee and V. M. Bolanos-Garcia (2015). "BubR1 kinase: protection against aneuploidy and premature aging." Trends Mol Med 21(6): 364-372.

Kiyomitsu, T., C. Obuse and M. Yanagida (2007). "Human Blinkin/AF15q14 is required for chromosome alignment and the mitotic checkpoint through direct interaction with Bub1 and BubR1." Dev Cell 13(5): 663-676.

Kruse, T., G. Zhang, M. S. Larsen, T. Lischetti, W. Streicher, T. Kragh Nielsen, S. P. Bjorn and J. Nilsson (2013). "Direct binding between BubR1 and B56-PP2A phosphatase complexes regulate mitotic progression." J Cell Sci 126(Pt 5): 1086-1092.

Kulukian, A., J. S. Han and D. W. Cleveland (2009). "Unattached kinetochores catalyze production of an anaphase inhibitor that requires a Mad2 template to prime Cdc20 for BubR1 binding." Dev Cell 16(1): 105-117.

Lampson, M. A. and I. M. Cheeseman (2011). "Sensing centromere tension: Aurora B and the regulation of kinetochore function." Trends Cell Biol 21(3): 133-140.

Lampson, M. A. and T. M. Kapoor (2005). "The human mitotic checkpoint protein BubR1 regulates chromosome-spindle attachments." Nat Cell Biol 7(1): 93-98.

Lara-Gonzalez, P., M. I. Scott, M. Diez, O. Sen and S. S. Taylor (2011). "BubR1 blocks substrate recruitment to the APC/C in a KEN-box-dependent manner." J Cell Sci 124(Pt 24): 4332-4345.

Lara-Gonzalez, P., F. G. Westhorpe and S. S. Taylor (2012). "The spindle assembly checkpoint." Curr Biol 22(22): R966-980.

Larsen, N. A., J. Al-Bassam, R. R. Wei and S. C. Harrison (2007). "Structural analysis of Bub3 interactions in the mitotic spindle checkpoint." Proc Natl Acad Sci U S A 104(4): 1201-1206.

Lee, H., A. H. Trainer, L. S. Friedman, F. C. Thistlethwaite, M. J. Evans, B. A. Ponder and A. R. Venkitaraman (1999). "Mitotic checkpoint inactivation fosters transformation in cells lacking the breast cancer susceptibility gene, BRCA2." Mol Cell 4(1): 1-10.

Lee, M., M. J. Daniels and A. R. Venkitaraman (2004). "Phosphorylation of BRCA2 by the Polo-like kinase Plk1 is regulated by DNA damage and mitotic progression." Oncogene 23(4): 865-872.

Lin, H. R., N. S. Ting, J. Qin and W. H. Lee (2003). "M phase-specific phosphorylation of BRCA2 by Polo-like kinase 1 correlates with the dissociation of the BRCA2-P/CAF complex." J Biol Chem 278(38): 35979-35987.

Lischetti, T., G. Zhang, G. G. Sedgwick, V. M. Bolanos-Garcia and J. Nilsson (2014). "The internal Cdc20 binding site in BubR1 facilitates both spindle assembly checkpoint signalling and silencing." Nat Commun 5: 5563.

Liu, D., O. Davydenko and M. A. Lampson (2012). "Polo-like kinase-1 regulates kinetochore-microtubule dynamics and spindle checkpoint silencing." J Cell Biol 198(4): 491-499.

Liu, D., M. Vleugel, C. B. Backer, T. Hori, T. Fukagawa, I. M. Cheeseman and M. A. Lampson (2010). "Regulated targeting of protein phosphatase 1 to

the outer kinetochore by KNL1 opposes Aurora B kinase." J Cell Biol 188(6): 809-820.

Maldonado, M. and T. M. Kapoor (2011). "Constitutive Mad1 targeting to kinetochores uncouples checkpoint signalling from chromosome biorientation." Nat Cell Biol 13(4): 475-482.

Malureanu, L. A., K. B. Jeganathan, M. HaMada, L. Wasilewski, J. Davenport and J. M. van Deursen (2009). "BubR1 N terminus acts as a soluble inhibitor of Cyclin B degradation by APC/C(Cdc20) in interphase." Dev Cell 16(1): 118-131.

Mansfeld, J., P. Collin, M. O. Collins, J. S. Choudhary and J. Pines (2011). "APC15 drives the turnover of MCC-CDC20 to make the spindle assembly checkpoint responsive to kinetochore attachment." Nat Cell Biol 13(10): 1234-1243.

Mao, Y., A. Abrieu and D. W. Cleveland (2003). "Activating and silencing the mitotic checkpoint through CENP-E-dependent activation/inactivation of BubR1." Cell 114(1): 87-98.

Matsumura, S., F. Toyoshima and E. Nishida (2007). "Polo-like kinase 1 facilitates chromosome alignment during prometaphase through BubR1." J Biol Chem 282(20): 15217-15227.

Mayer, T. U., T. M. Kapoor, S. J. Haggarty, R. W. King, S. L. Schreiber and T. J. Mitchison (1999). "Small molecule inhibitor of mitotic spindle bipolarity identified in a phenotype-based screen." Science 286(5441): 971-974.

Minshull, J., A. Straight, A. D. Rudner, A. F. Dernburg, A. Belmont and A. W. Murray (1996). "Protein phosphatase 2A regulates MPF activity and sister chromatid cohesion in budding yeast." Curr Biol 6(12): 1609-1620.

Mitchison, T. (2012). “The proliferation rate paradox in antimitotic chemotherapy.” Mol.Biol.Cell 23(1):1-6.

Musacchio, A. and E. D. Salmon (2007). "The spindle-assembly checkpoint in space and time." Nat Rev Mol Cell Biol 8(5): 379-393.

New, M., H. Olzscha and N. B. La Thangue (2012). "HDAC inhibitor-based

therapies: can we interpret the code?" Mol Oncol 6(6): 637-656.

Nilsson, J., M. Yekezare, J. Minshull and J. Pines (2008). "The APC/C maintains the spindle assembly checkpoint by targeting Cdc20 for destruction." Nat Cell Biol 10(12): 1411-1420.

Patel, K. J., V. P. Yu, H. Lee, A. Corcoran, F. C. Thistlethwaite, M. J. Evans, W. H. Colledge, L. S. Friedman, B. A. Ponder and A. R. Venkitaraman (1998). "Involvement of BRCA2 in DNA repair." Mol Cell 1(3): 347-357.

Pfleger, C. M. and M. W. Kirschner (2000). "The KEN box: an APC recognition signal distinct from the D box targeted by Cdh1." Genes Dev 14(6): 655-665.

Primorac, I., J. R. Weir, E. Chiroli, F. Gross, I. Hoffmann, S. van Gerwen, A. Ciliberto and A. MuSACchio (2013). "Bub3 reads phosphorylated MELT repeats to promote spindle assembly checkpoint signaling." Elife 2: e01030.

Rieder, C. L. (1981). "The structure of the cold-stable kinetochore fiber in metaphase PtK1 cells." Chromosoma 84(1): 145-158.

Santaguida, S., A. Tighe, A. M. D'Alise, S. S. Taylor and A. MuSACchio (2010). "Dissecting the role of MPS1 in chromosome biorientation and the spindle checkpoint through the small molecule inhibitor reversine." J Cell Biol 190(1): 73-87.

Santaguida, S., C. Vernieri, F. Villa, A. Ciliberto and A. MuSACchio (2011). "Evidence that Aurora B is implicated in spindle checkpoint signalling independently of error correction." EMBO J 30(8): 1508-1519.

Skoulidis, F., L. D. Cassidy, V. Pisupati, J. G. Jonasson, H. Bjarnason, J. E. Eyfjord, F. A. Karreth, M. Lim, L. M. Barber, S. A. Clatworthy, S. E. Davies, K. P. Olive, D. A. Tuveson and A. R. Venkitaraman (2010). "Germline BRCA2 heterozygosity promotes Kras(G12D) -driven carcinogenesis in a murine model of familial pancreatic cancer." Cancer Cell 18(5): 499-509.

Stevens, F. E., H. Beamish, R. Warrener and B. Gabrielli (2008). "Histone deacetylase inhibitors induce mitotic slippage." Oncogene 27(10): 1345-1354.

Sudakin, V., G. K. Chan and T. J. Yen (2001). "Checkpoint inhibition of the APC/C in HeLa cells is mediated by a complex of BUBR1, BUB3, CDC20,

and MAD2." J Cell Biol 154(5): 925-936.

Suijkerbuijk, S. J., T. J. van Dam, G. E. Karagoz, E. von Castelmur, N. C. Hubner, A. M. Duarte, M. Vleugel, A. Perrakis, S. G. Rudiger, B. Snel and G. J. Kops (2012). "The vertebrate mitotic checkpoint protein BUBR1 is an unusual pseudokinase." Dev Cell 22(6): 1321-1329.

Taddei, A., C. Maison, D. Roche and G. Almouzni (2001). "Reversible disruption of pericentric heterochromatin and centromere function by inhibiting deacetylases." Nat Cell Biol 3(2): 114-120.

Takaoka, M., H. Saito, K. Takenaka, Y. Miki and A. Nakanishi (2014). "BRCA2 phosphorylated by PLK1 moves to the midbody to regulate cytokinesis mediated by nonmuscle myosin IIC." Cancer Res 74(5): 1518-1528.

Taylor, S. S., E. Ha and F. McKeon (1998). "The human homologue of Bub3 is required for kinetochore localization of Bub1 and a Mad3/Bub1-related protein kinase." J Cell Biol 142(1): 1-11.

Teichner, A., E. Eytan, D. Sitry-Shevah, S. Miniowitz-Shemtov, E. Dumin, J. Gromis and A. Hershko (2011). "p31comet Promotes disassembly of the mitotic checkpoint complex in an ATP-dependent process." Proc Natl Acad Sci U S A 108(8): 3187-3192.

Uchida, K. S., K. Takagaki, K. KuMada, Y. Hirayama, T. Noda and T. Hirota (2009). "Kinetochore stretching inactivates the spindle assembly checkpoint." J Cell Biol 184(3): 383-390.

Venkitaraman, A. R. (2014). "Cancer suppression by the chromosome custodians, BRCA1 and BRCA2." Science 343(6178): 1470-1475.

Wang, E., E. R. Ballister and M. A. Lampson (2011). "Aurora B dynamics at centromeres create a diffusion-based phosphorylation gradient." J Cell Biol 194(4): 539-549.

Wang, F., N. P. Ulyanova, J. R. Daum, D. Patnaik, A. V. Kateneva, G. J. Gorbsky and J. M. Higgins (2012). "Haspin inhibitors reveal centromeric functions of Aurora B in chromosome segregation." J Cell Biol 199(2): 251-268.

Warrener, R., K. Chia, W. D. Warren, K. Brooks and B. Gabrielli (2010).

"Inhibition of histone deacetylase 3 produces mitotic defects independent of alterations in histone H3 lysine 9 acetylation and methylation." Mol Pharmacol 78(3): 384-393.

Westhorpe, F. G., A. Tighe, P. Lara-Gonzalez and S. S. Taylor (2011). "p31comet-mediated extraction of Mad2 from the MCC promotes efficient mitotic exit." J Cell Sci 124(Pt 22): 3905-3916.

Wu, J. Q., J. Y. Guo, W. Tang, C. S. Yang, C. D. Freel, C. Chen, A. C. Nairn and S. Kornbluth (2009). "PP1-mediated dephosphorylation of phosphoproteins at mitotic exit is controlled by inhibitor-1 and PP1 phosphorylation." Nat Cell Biol 11(5): 644-651.

Yang, M., B. Li, D. R. Tomchick, M. Machius, J. Rizo, H. Yu and X. Luo (2007). "p31comet blocks Mad2 activation through structural mimicry." Cell 131(4): 744-755.

Yang, Z., A. E. Kenny, D. A. Brito and C. L. Rieder (2009). "Cells satisfy the mitotic checkpoint in Taxol, and do so faster in concentrations that stabilize syntelic attachments." J Cell Biol 186(5): 675-684.

Zhou, L., X. Tian, C. Zhu, F. Wang and J. M. Higgins (2014). "Polo-like kinase-1 triggers histone phosphorylation by Haspin in mitosis." EMBO Rep 15(3): 273-281.

국문 초록

BubR1은 세포분열 복합체 (MCC)를 구성하는 중요 단백질로, APC/C E3 리가아제 활성을 조절하여 세포분열 체크포인트(SAC)를 관장한다. 본 연구는 1) BubR1이 염색체 방추사 부착점에 미세소관의 부착과 세포분열 체크포인트 신호 전달을 어떻게 조절하는지, 그리고 2) 세포분열 체크포인트에서도 작용한다고 알려진 암 억제인자 BRCA2가 기존의 세포분열기에서의 역할에서 더 나아가 신호전달 지지체로 활발하게 작용한다는 내용을 포함하고 있다.

BubR1의 아세틸화가 생리학적으로 어떠한 의미를 가는지 분석하기 위해 아세틸화가 결손 된 마우스(*K243R/+*)를 knock-in 방법을 이용하여 제작하였다. 약 60주가 지나면 38%의 개체의 다양한 조직에서 자연적으로 암이 발생하였다. 해당 마우스의 세포를 분석한 결과, 염색체 이수성이 높게 나타났으며, 세포분열 체크포인트도 약화되어있었다. BubR1 아세틸화가 저해된 세포의 염색체 방추사 부착점에서는 PP2AB56a가 적게 형성되고, Aurora B가 활성화되는 문제로 미세소관 부착이 불안정하였다. 즉, BubR1 아세틸화가 1) MMC 복합체 유지와 2) 염색체 방추사 부착점과 미세소관 사이의 안정적 결합을 형성하는데 중요하게 작용하고, 이 두 특성이 *K243R/+* 마우스에서는 저해되어 있어 염색체 불안정성(CIN)이 축적되었다고 볼 수 있다. CIN은 세포분열이 여러 번 반복되면서 다양한 형태로 나타났으며, 실제 암 발생과 연관성이 높고, 영향을

줄 수 있다고 알려진 유전자 돌연변이를 유도하였다.

사전 연구결과들은 염색체 분열기가 시작될 때 염색체 방추사 부착점에서 BRCA2의 매개로 BubR1이 PCAF에 의해 아세틸화된다는 것을 보여주었다. 본 연구에서는 염색체 분열기가 종료될 때, 즉 세포분열 체크포인트가 비활성화될때 BubR1의 탈아세틸화가 필수임을 보여준다. BubR1의 탈아세틸화는 세포분열 체크포인트 비활성화에 작용하는데, 이는 BubR1 아세틸화가 지속적으로 유지되면 중기가 오래 지속되면서 세포분열이 완료되지 않는 것으로 확인할 수 있었다. 또한, 생화학적으로 세포분열기에 들어가 있는 세포에서 세포분열 체크포인트 신호를 억제하여 세포분열 체크포인트가 비활성화된 상황을 재현하였을 때 BubR1의 탈아세틸화가 진행되는 것을 보였다. BubR1의 탈아세틸화는 class I 탈아세틸화 효소 (HDAC)에 의해 조절되며, 해당 작용에는 BRCA2가 탈아세틸화 효소와 BubR1의 결합 형성에 필요하였다. 따라서, BRCA2는 기존에 알려진 BubR1의 아세틸화 뿐만 아니라 더 나아가 세포분열기 BubR1의 탈아세틸화에도 작용한다고 볼 수 있다. 세포분열기에서의 BRCA2 복합체 분석을 통해 BRCA2가 세포분열 체크포인트 신호전달 과정에서 특정 단백질들이 염색체 동원체 부착점에 위치하고 서로간의 결합을 형성할 수 있게 도와주면서, 하나의 신호전달 지지체로 작용할 수 있음을 제안하고자 한다.

결과적으로 해당 연구 내용은 세포분열 연구에서 대두되는 중요 질문들에 대한 답을 제시함으로써 이해를 증진시켰다고 볼

수 있다. 첫째, 염색체 동원체 부착점에 방추사가 부착되면서 나타나는 물리적 변화가 어떻게 SAC 조절에 필요한 화학적 시그널로 변화하는지는 BubR1이 염색체 부착점과 방추사 연결, 그리고 SAC 조절에 연계하여 작용하는 점으로 설명하고 있다. 둘째, 짧은 시간 안에 어떻게 SAC 신호전달이 효율적으로 작용할 수 있는지에 대해서는 BRCA2가 BubR1 아세틸/탈아세틸화 조절에 지지체로 작용한다는 점으로 설명하고 있다.

주요어: 세포분열 체크포인트, BubR1, 암 발생, 세포분열 체크포인트 신호 전달, 동원체-방추사 부착

학생 번호: 2011-20330